

# RIS-Assisted Multihop FSO/RF Hybrid System for Vehicular Communications over Generalized Fading

Vinay Kumar Chapala, *Graduate Student Member, IEEE* and S. M. Zafaruddin, *Senior Member, IEEE*

**Abstract**—Reconfigurable intelligent surface (RIS) is a promising technology to avoid signal blockage by creating line-of-sight (LOS) connectivity for free-space optical (FSO) and radio frequency (RF) wireless systems. There is limited research on the use of multiple RIS between a source and destination for wireless communications. This paper analyzes the performance of a RIS-assisted multi-hop transmission for vehicular communications by employing multiple RIS to enable LOS communication and reliable connectivity for a hybrid FSO and RF system. We develop an analytical framework to derive statistical results of the signal-to-noise ratio (SNR) of a multi-RIS communication system over general fading models. We use decode-and-forward (DF) and fixed-gain (FG) relaying protocols to mix multi-RIS transmissions over RF and FSO technologies, and derive probability density and distribution functions for both the relaying schemes by considering independent and non-identical double generalized gamma (dGG) distribution models for vehicular RF transmissions and atmospheric turbulence for FSO system combined with zero-boresight pointing errors. We analyze the performance of a moving vehicle connected to one of the RIS modules by deriving exact analytical expressions of the outage probability, average bit-error rate (BER), and ergodic capacity in terms of Fox's H-function. We present asymptotic analysis and diversity order of the outage probability in the high SNR regime to provide a better insight into the system performance. We use computer simulations to demonstrate the effect of multiple RIS modules, fading parameters, and pointing errors on the RIS-aided multi-hop transmissions for the considered vehicular communication system.

**Index Terms**—Bit error rate, ergodic rate, Fox-H function, multihop, multi RIS, outage probability, performance analysis, reconfigurable intelligent surface (RIS), relaying, vehicular communications.

## I. INTRODUCTION

Reconfigurable intelligent surface (RIS) is emerging as a disruptive technology for wireless and vehicular communications [1]–[4]. RISs are artificial planar structures of metasurfaces, intelligently programmed to control electromagnetic waves in the desired direction. A single RIS module can contain hundreds of elements, each sub-wavelength size, to beamform the signal for enhanced performance without requiring expensive relaying procedures. In recent years, free-space optical (FSO) for backhaul/fronthaul and radio frequency (RF) for broadband access have been considered as a potential architecture for next generation wireless communications [5].

The FSO is a line-of-sight (LOS) technology with a higher unlicensed optical spectrum, which can be employed for secured high data rate transmissions. The RIS can assist FSO and RF transmissions to resolve the problem of signal blockage for enhanced performance for terrestrial and vehicular communications.

There has been an increased research interest to assess the applicability of RIS based wireless systems for intelligent vehicular communications [6]–[15], radio-frequency (RF) [16]–[24], free-space-optics (FSO) [25]–[30], and terahertz (THz) wireless systems [31]–[33]. The authors in [9] applied series expansion and central limit theorem (CLT) to approximate the outage probability performance of the RIS-assisted vehicular communication assuming Rayleigh and Rician fading channels. In [11], the authors provided an approximate analysis on the outage probability and effective rate for RIS-assisted V2V communications over Fox's-H function by approximating the distribution of the signal-to-noise ratio (SNR) of the resultant channel as a mixture of Gaussian distributions. The authors in [12] evaluated the performance of RIS-enabled vehicular system considering joint impact of Fisher-Snedecor ( $\mathcal{F}$ ) fading channel and the vehicle mobility modeled as a random way point. In [10], the authors optimized the data rate performance for the uplink transmission by reducing the channel estimation overhead for each reflecting element of the RIS module. The use of RIS has also been investigated for physical layer secured V2V systems [6]–[8] and in the context of resource allocation for RIS-aided vehicular communications [13].

In the aforementioned and related research, a single RIS module has been employed for vehicular communications. However, the deployment of multiple RIS units is highly desirable for reliable connectivity for moving vehicles. The authors in [34] developed algorithms for optimum placement of multiple RISs for a roadside deployment scenario considering the size and operating modes of RISs for vehicle-to-everything (V2X) connectivity. To further substantiate, it is desirable to analyze the performance metrics such as outage probability, average BER, and ergodic capacity of multiple RIS based vehicular communications over fading channels. In [35], the authors proposed a deep reinforcement learning (DRL) based hybrid beamforming for multi-hop RIS-empowered terahertz system with Rician fading channel to improve the coverage range at terahertz-band frequencies. Recently, the authors in [36] analyzed the system performance of a multi-hop RIS assisted FSO system considering Gamma-Gamma atmospheric turbulence with pointing errors. They modeled the multi-RIS as a cascaded system, and used the mathematical induction method to derive the probability density function (PDF) and

Vinay Kumar Chapala (p20200110@pilani.bits-pilani.ac.in) and S. M. Zafaruddin (syed.zafaruddin@pilani.bits-pilani.ac.in) are with the Department of Electrical and Electronics Engineering, Birla Institute of Technology and Science, Pilani, Pilani-333031, Rajasthan, India.

This work was supported in part by the Science and Engineering Research Board (SERB), Department of Science and Technology (DST), Government of India, under Start-up Research Grant SRG/2019/002345.

cumulative distribution function (CDF) of the Gamma-Gamma fading channel and zero-boresight pointing errors. However, the induction method may not be applicable readily for other atmospheric turbulence and RF fading distributions such as double generalized Gamma (dGG) [37], [38]. The dGG model is suitable for modeling non-homogeneous double-scattering radio propagation fading conditions for V2V communications over RF frequencies [38]. Further, the dGG distribution for the atmospheric turbulence in FSO system is superior to the Gamma-Gamma model since the dGG model is valid under all range of turbulence conditions (weak to strong) for both plane and spherical waves propagation [37], [39]–[41]. The dGG is a generalized model which contains most of the existing statistical models such as double-Nakagami, double-Rayleigh, double Weibull, and Gamma-Gamma as special cases.

There has been some study on the performance of a single RIS assisted mixed FSO-RF systems [42]–[45]. In [42]–[44], the authors used the decode-and-forward (DF) relaying to mix an FSO link over Gamma-Gamma turbulence with a RIS-assisted RF link over Rayleigh fading. In [44], authors analyzed the performance of a RIS-equipped source mixed RF/FSO system by considering RIS located close to the source in the RF link. It should be mentioned that fixed-gain amplify-and-forward (AF) relaying is well acknowledged for its desirable characteristics of lower computational complexity and the fact that it does not require continuous channel monitoring for decoding at the relay [46]. Further, deriving analytical results for fixed-gain relaying with generalized fading models is challenging compared with the DF protocol. The authors in [45] investigated the outage probability performance of a fixed-gain relayed system for the mixed visible light communication (VLC)-RF with VLC in the first link and a single RIS module in the second RF link for an indoor environment. To the best of authors' knowledge, a multiple RIS empowered mixed FSO-RF relayed system over dGG fading channels has not been reported in the literature.

In this paper, we analyze the performance of a mixed FSO-RF system by employing multiple RISs in both the links for multi-hop transmissions for reliable connectivity of moving vehicles. We assume the dGG turbulence model and zero-boresight pointing errors for the FSO link and the dGG distribution to model the signal fading for vehicular transmissions over RF. The major contributions of the paper are listed as follows:

- We develop an analytical framework to derive density and distribution functions of the end-to-end SNR of a multi-RIS communication system over a general fading model.
- We derive PDF and CDF of the fixed-gain (FG) relaying to mix multi-RIS empowered vehicular transmissions over RF and FSO backhaul with zero-boresight pointing errors considering independent and non-identical (i.n.i.d) double generalized gamma (dGG) distribution function without any constraint on its parameters. It is noted that the existing representation of the PDF of the dGG model requires the ratio of shape parameters to be an integer for the performance analysis of FSO systems [39], [40] and equal shape parameters for the statistical analysis of V2V communications [38].

- We analyze the performance of the AF-assisted system by deriving exact analytical expressions of the outage probability, average bit-error-rate (BER), and ergodic capacity in terms of bivariate Fox's H-function. We also analyze the performance by integrating the FSO and RF systems using decode-and-forward (DF) relaying in terms of single-variate Fox's H-function.
- We present asymptotic analysis in the high SNR regime for outage probability and average BER in terms of simpler Gamma functions, and derive diversity order depicting the impact of fading parameters on the performance of the considered system.
- We use computer simulations to demonstrate the performance of the multi-hop system and validate the accuracy of derived analytical expressions through Monte-Carlo simulations for various fading scenarios.

## II. SYSTEM MODEL

We consider a hybrid multi-hop FSO/RF system assisted by multiple RISs in both transmission links as shown in Fig. 1. The source ( $S$ ) intends to transmit signals for a moving vehicle ( $V$ ). We consider a communication link comprising of backhaul/fronthaul on FSO technology and vehicular link on the RF. A relay ( $R$ ) with the functionality of AF/DF is deployed to integrate the FSO and RF technologies. The relay is equipped with a photodetector for receiving FSO signals and a frequency down-converter for low frequency RF communications. We employ multiple optical RIS to assist the communication from the source to the relay since there is no direct link between them for the line-of-sight FSO transmissions. Thus, the source communicates data to the relay through  $K_1$  hops using  $K_1 - 1$  optical RIS modules. The use of multiple RIS for vehicular communications over RF is more appealing since a direct link from the relay to the destination vehicle (R2V) is not possible due to other vehicles on the road. We employ  $K_2 - 1$  RF RIS modules perpendicular to the road such that the desired vehicle is connected to one of the RIS modules.

We assume that each optical RIS reflects the incident beam towards subsequent optical RIS until the last RIS directs the beam towards the relay. In a recent paper [47], a different system configuration has been considered by employing multiple RIS such that the destination directly receives signals from each RIS independent of other RIS. Thus, the received signal  $y_R$  at the relay is given by

$$y_R = h_{S,1} \prod_{j=1}^{K_1-2} h_{j,j+1} h_{K_1-1,R} s + w_R \quad (1)$$

where  $s$  is the transmitted signal of source with power  $P$ ,  $w_R$  is the additive white Gaussian noise (AWGN) with variance  $\sigma_R^2$ ,  $h_{S,1}$  is the channel coefficient from the source to the first-optical RIS,  $h_{j,j+1}$  is the channel from  $j$ -th optical RIS to  $(j+1)$ -optical RIS, and  $h_{K_1-1,R}$  is the channel coefficient of last  $(K_1 - 1)$ -optical RIS to relay.

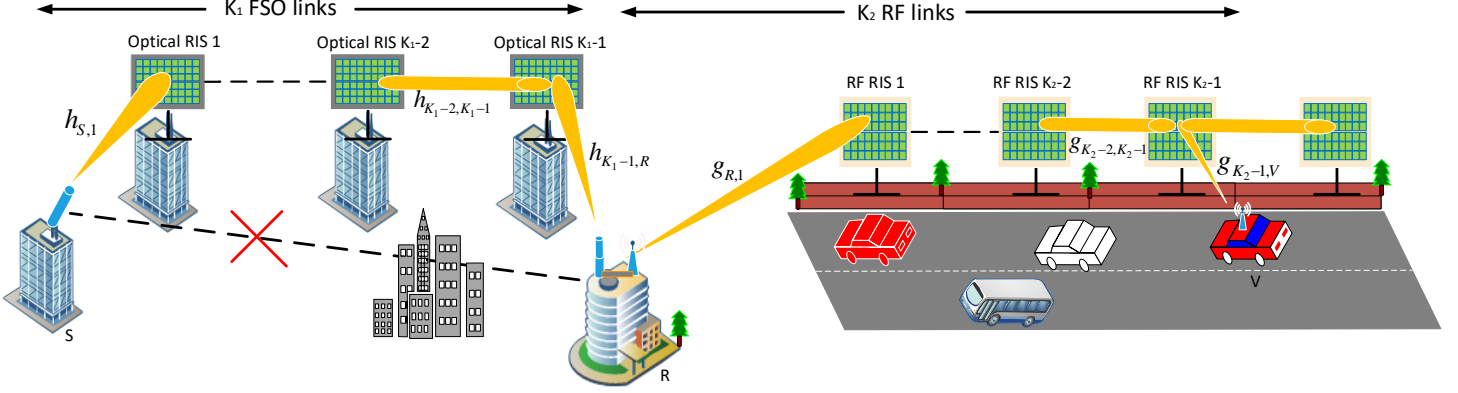


Fig. 1: Schematic diagram of a multiple RIS empowered vehicular communications.

Similarly, the received signal at destination vehicle connected through  $(K_2 - 1)$ -th RIS is given by

$$y = g_{S,1} \prod_{j=1}^{K_2-2} g_{j,j+1} g_{K_2-1,V} s + w_V \quad (2)$$

where  $w_V$  is the additive white Gaussian noise (AWGN) at the destination with variance  $\sigma_V^2$ ,  $g_{S,1}$  is the channel coefficient from the relay to the first RIS,  $g_{j,j+1}$  is the channel from  $j$ -th RIS to  $(j+1)$ -RIS, and  $g_{K_2-1,V}$  is the channel coefficient of the last  $(K_2 - 1)$ -RIS to destination vehicle.

We consider the dGG distribution to model the atmospheric turbulence for the FSO and multi-path fading for the RF link. As such, the dGG is the product of two generalized Gamma functions. The PDF of a generalized Gamma function is given as

$$f_{\chi}(x) = \frac{\alpha x^{\alpha\beta-1}}{(\frac{\Omega}{\beta})^{\beta} \Gamma(\beta)} \exp\left(-\frac{\beta}{\Omega} x^{\alpha}\right) \quad (3)$$

where  $\alpha, \beta$  are Gamma distribution shaping parameters and  $\Omega = (\frac{\mathbb{E}[\chi^2] \Gamma(\beta)}{\Gamma(\beta+2/\alpha)})^{\alpha/2}$  is the  $\alpha$ -root mean value.

In addition to the atmospheric turbulence, we consider pointing errors in each hop of the FSO link such that the combined channel fading is  $h_{i,j} = h_{i,j}^{(l)} h_{i,j}^{(t)} h_{i,j}^{(p)}$ , where subscripts  $(l)$ ,  $(t)$  and  $(p)$  denote path loss, atmospheric turbulence and pointing error fading coefficients. To characterize pointing errors statistically, we use the recently proposed model for optical RIS in [27], which is based on the zero-boresight model [48]:

$$f_{h_{i,j}^{(p)}}(x) = \frac{\rho^2}{A_0^{\rho^2}} x^{\rho^2-1}, 0 \leq x \leq A_0, \quad (4)$$

where the term  $A_0 = \text{erf}(v)^2$  denotes the fraction of collected power. Define  $v = \sqrt{\pi/2} a_r / \omega_z$  with  $a_r$  as the aperture radius and  $\omega_z$  as the beam width. We define the term  $\rho^2 = \frac{\omega_{z_{\text{eq}}}^2}{\xi}$  where  $\omega_{z_{\text{eq}}}$  is the equivalent beam width at the receiver. The use of  $\xi = 4\sigma_{\theta}^2 d_1^2 + 16\sigma_{\beta}^2 d_2^2$  models the pointing errors for the RIS-FSO system, where  $\sigma_{\theta}$  and  $\sigma_{\beta}$  represent pointing error and RIS jitter angle standard deviation defined in [27].

Similarly, we denote the channel coefficient between the  $i$ -th and  $j$ -th RIS as  $g_{i,j} = g_{i,j}^{(l)} g_{i,j}^{(f)}$ , where subscripts  $(l)$  and  $(f)$  denote path loss and short-term fading coefficients of RF links. Note that the path-loss  $g_{K_2-1,V}^{(l)}$  between the RIS and destination vehicle is random considering the movement of the vehicle.

### III. STATISTICAL RESULTS FOR CASCADED CHANNELS

To facilitate the performance analysis, we require density and distribution functions of the cascaded FSO channels  $h = \prod_{i=1}^{K_1} h_i = \prod_{i=1}^{K_1} h_i^{(t)} h_i^{(p)}$  and cascaded RF channels  $g = \prod_{i=1}^{K_2} g_i$ . In the following two propositions, we express the PDF of dGG  $g_i$  and product of dGG with pointing errors  $h_i$  in terms of Fox-H function to remove the constraint of integer-valued fading parameter manifestation of Meijer-G representation [37], [39] and equal shape parameters for the statistical analysis of V2V communications [38].

**Proposition 1.** The PDF of double generalized-gamma  $g_i = \chi_1 \chi_2$ , where  $\chi_1 \sim \mathcal{GG}(\alpha_1, \beta_1, \Omega_1)$  and  $\chi_2 \sim \mathcal{GG}(\alpha_2, \beta_2, \Omega_2)$  is given by

$$f_{g_i}(x) = \frac{x^{\alpha_2 \beta_2 - 1}}{(\frac{\Omega_1}{\beta_1})^{\frac{\alpha_2 \beta_2}{\alpha_1}} (\frac{\Omega_2}{\beta_2})^{\beta_2} \Gamma(\beta_1) \Gamma(\beta_2)} H_{0,2}^{2,0} \left[ \psi x \mid \left(0, \frac{1}{\alpha_2}\right), \left(\frac{\alpha_1 \beta_1 - \alpha_2 \beta_2}{\alpha_1}, \frac{1}{\alpha_1}\right) \right] \quad (5)$$

where  $\psi = (\frac{\beta_2}{\Omega_2})^{\frac{1}{\alpha_2}} (\frac{\beta_1}{\Omega_1})^{\frac{1}{\alpha_1}}$ .

*Proof:* Using the PDF of the product of two random variables  $f_{g_i}(x) = \int_0^\infty \frac{1}{u} f_{\chi_1}(\frac{x}{u}) f_{\chi_2}(u) du$

$$f_{g_i}(x) = \frac{\alpha_1 \alpha_2 x^{\alpha_1 \beta_1 - 1}}{(\frac{\Omega_1}{\beta_1})^{\beta_1} (\frac{\Omega_2}{\beta_2})^{\beta_2} \Gamma(\beta_1) \Gamma(\beta_2)} \int_0^\infty u^{\alpha_2 \beta_2 - \alpha_1 \beta_1 - 1} \exp\left(-\frac{\beta_1 x^{\alpha_1}}{\Omega_1} u^{-\alpha_1}\right) \exp\left(-\frac{\beta_2}{\Omega_2} u^{\alpha_2}\right) du \quad (6)$$

Using  $u^{-\alpha_1} = t$ , and representing the exponential function using Meijer-G, we get

$$f_{g_i}(x) = \frac{\alpha_2 x^{\alpha_1 \beta_1 - 1}}{(\frac{\Omega_1}{\beta_1})^{\beta_1} (\frac{\Omega_2}{\beta_2})^{\beta_2} \Gamma(\beta_1) \Gamma(\beta_2)} \int_0^\infty t^{\frac{\alpha_1 \beta_1 - \alpha_2 \beta_2}{\alpha_1} - 1} G_{0,1}^{1,0} \left[ \frac{\beta_1 x^{\alpha_1}}{\Omega_1} t \mid - \right] G_{1,0}^{0,1} \left[ \frac{\Omega_2 t^{\frac{\alpha_2}{\alpha_1}}}{\beta_2} \mid - \right] dt \quad (7)$$

Applying identity [49, 07.34.21.0012.01] in (7), we get (5). ■

The derived PDF in (5) does not have any constraint on the parameters of dGG as present in the Meijer's-G representation [37]. It should be mentioned that the use of Fox's-H function for performance analysis is becoming popular similar to the Meijer's-G function. Recently MATHEMATICA introduced FoxH function for the computation of single-variate Fox's-H function.

Next, we derive the PDF of the FSO link with the combined effect of dGG atmospheric turbulence and pointing errors:

**Proposition 2.** *If the pointing error parameter  $h_p$  is distributed according to (4), then the PDF of the single FSO link  $h_i = g_i h_p$  with the combined effect of dGG and pointing errors is given by*

$$f_{h_i}(x) = \frac{\rho^2 x^{\alpha_2 \beta_2 - 1}}{A_0^{\alpha_1 \beta_2} (\frac{\Omega_1}{\beta_1})^{\frac{\alpha_2 \beta_2}{\alpha_1}} (\frac{\Omega_2}{\beta_2})^{\beta_2} \Gamma(\beta_1) \Gamma(\beta_2)} H_{1,3}^{3,0} \left[ \frac{\psi x}{A_0} \mid (0, \frac{1}{\alpha_{i,2}}), (\frac{\rho^2 - \alpha_2 \beta_2 + 1}{\alpha_1}, \frac{1}{\alpha_1}), (\rho^2 - \alpha_2 \beta_2, 1) \right] \quad (8)$$

where  $\psi = (\frac{\beta_2}{\Omega_2})^{\frac{1}{\alpha_2}} (\frac{\beta_1}{\Omega_1})^{\frac{1}{\alpha_1}}$ .

*Proof:* The combined PDF of dGG and pointing error can be expressed as

$$f_{h_i}(x) = \int_0^{A_0} \frac{1}{u} f_{\chi}(\frac{x}{u}) f_{h_p}(u) du \quad (9)$$

Substituting (5) and (4) in (9) with the definition of Fox-H function and interchanging the integrals as per Fubini's theorem to get

$$f_{h_i}(x) = \frac{\alpha_2 x^{\alpha_2 \beta_2 - 1}}{(\frac{\Omega_1}{\beta_1})^{\frac{\alpha_2 \beta_2}{\alpha_1}} (\frac{\Omega_2}{\beta_2})^{\beta_2} \Gamma(\beta_1) \Gamma(\beta_2)} \frac{\rho^2}{A_0^{\rho^2}} \frac{1}{2\pi j} \int_{\mathcal{L}} \Gamma(-s) \Gamma(\frac{\alpha_1 \beta_1 - \alpha_2 \beta_2}{\alpha_1} - \frac{\alpha_2}{\alpha_1} s) \left( \frac{\beta_2}{\Omega_2} (\frac{\beta_1}{\Omega_1})^{\frac{\alpha_2}{\alpha_1}} (x)^{\alpha_2} \right)^s \left( \int_0^{A_0} u^{\rho^2 - \alpha_2 \beta_2 - \alpha_2 s - 1} du \right) ds \quad (10)$$

The inner integral of (10) is solved as  $\int_0^{A_0} u^{\rho^2 - \alpha_2 \beta_2 - \alpha_2 s - 1} du = \frac{A_0^{\rho^2 - \alpha_2 \beta_2 - \alpha_2 s}}{\rho^2 - \alpha_2 \beta_2 - \alpha_2 s} = A_0^{\rho^2 - \alpha_2 \beta_2 - \alpha_2 s} \frac{\Gamma(\rho^2 - \alpha_2 \beta_2 - \alpha_2 s)}{\Gamma(\rho^2 - \alpha_2 \beta_2 - \alpha_2 s + 1)}$ . We substitute the inner integral in (10), and apply the definition of Fox-H with the identity [50, 1.59] to get (8). ■

We validate the derived PDF in (8) by integrating  $\int_0^\infty f_{h_i}(x) dx$  to show that

$$= \frac{\rho^2 \Gamma(\beta_2) \Gamma(\beta_1)}{(\frac{\Omega_1}{\beta_1})^{\frac{\alpha_2 \beta_2}{\alpha_1}} (\frac{\Omega_2}{\beta_2})^{\beta_2} \Gamma(\beta_1) \Gamma(\beta_2)} \frac{\Gamma(\rho^2)}{\Gamma(\rho^2 + 1)} \left( \frac{\beta_2}{\Omega_2} (\frac{\beta_1}{\Omega_1})^{\frac{\alpha_2}{\alpha_1}} \right)^{-\beta_2} = 1 \quad (11)$$

Note that PDF of [39] is a special case of the Fox-H representation of the derived PDF in (8).

Finally, we develop a unifying framework to derive the PDF and CDF of cascaded channels  $h$  and  $g$  in the following Theorem:

**Theorem 1.** *If  $X_i$ ,  $i = 1 \dots K$  are i.n.i.d random variables with a PDF of the form*

$$f_{X_i}(x) = \psi_i x^{\phi_i - 1} H_{p,q}^{m,n} \left[ \zeta_i x \mid \frac{\{(a_{i,j}, A_{i,j})\}_{j=1}^p}{\{(b_{i,j}, B_{i,j})\}_{j=1}^q} \right] \quad (12)$$

then the PDF and CDF of  $X = \prod_{i=1}^K X_i$  are given by

$$f_X(x) = \frac{1}{x} \prod_{i=1}^K \psi_i \zeta_i^{-\phi_i} H_{Kp, Kq}^{Km, Kn} \left[ \prod_{i=1}^K \zeta_i x \mid \frac{\{\{(a_{i,j} + A_{i,j} \phi_i, A_{i,j})\}_{j=1}^p\}_{i=1}^K}{\{\{(b_{i,j} + B_{i,j} \phi_i, B_{i,j})\}_{j=1}^q\}_{i=1}^K} \right] \quad (13)$$

$$F_X(x) = \prod_{i=1}^K \psi_i \zeta_i^{-\phi_i} H_{Kp+1, Kq+1}^{Km, Kn+1} \left[ \prod_{i=1}^K \zeta_i x \mid \frac{(1, 1), \{\{(a_{i,j} + A_{i,j} \phi_i, A_{i,j})\}_{j=1}^p\}_{i=1}^K}{\{(b_{i,j} + B_{i,j} \phi_i, B_{i,j})\}_{j=1}^q\}_{i=1}^K, (0, 1)} \right] \quad (14)$$

*Proof:* See Appendix A. ■

In what follows, we capitalize Theorem 1 to present the PDF and CDF of the cascaded FSO and vehicular channels realized through multiple RIS modules:

**Corollary 1.** *If  $h_i$  is distributed according to (8), the PDF and CDF of cascaded FSO channel  $h = \prod_{i=1}^{K_1} h_i$  are*

$$f_h(x) = \frac{1}{x} \psi_1 H_{K_1+1, 3K_1}^{3K_1, 0} \left[ U_1 x \mid \frac{\{(\rho_i^2 + 1, 1)\}_{i=1}^{K_1}}{V_1} \right] \quad (15)$$

$$F_h(x) = \psi_1 H_{K_1+1, 3K_1+1}^{3K_1, 1} \left[ U_1 x \mid \frac{(1, 1), \{(\rho_i^2 + 1, 1)\}_{i=1}^{K_1}}{V_1, (0, 1)} \right] \quad (16)$$

where  $\psi_1 = \prod_{i=1}^{K_1} \frac{\rho_i^2}{\Gamma(\beta_{i,1}) \Gamma(\beta_{i,2})}$ ,  $U_1 = \prod_{i=1}^{K_1} \frac{1}{A_{0,i}} (\frac{\beta_{i,2}}{\Omega_{i,2}})^{\frac{1}{\alpha_{i,2}}} (\frac{\beta_{i,1}}{\Omega_{i,1}})^{\frac{1}{\alpha_{i,1}}}$  and  $V_1 = \{(\beta_{i,1}, \frac{1}{\alpha_{i,1}}), (\beta_{i,2}, \frac{1}{\alpha_{i,2}}), (\rho_i^2, 1)\}_{i=1}^{K_1}$ .

*Proof:* A straight forward application of Theorem 1 proves the Corollary 1. ■

To prove  $\int_0^\infty f_h(x) dx = 1$ , we use the identity [50, 2.8]

$$\int_0^\infty f_h(x) dx = \psi_1 \int_0^\infty x^{-1} H_{K_1+1, 3K_1}^{3K_1, 0} \left[ U_1 x \mid \frac{\{(\rho_i^2 + 1, 1)\}_{i=1}^{K_1}}{V_1} \right] dx = \prod_{i=1}^{K_1} \frac{\rho_i^2}{\Gamma(\beta_{i,1}) \Gamma(\beta_{i,2})} \prod_{i=1}^{K_1} \frac{\Gamma(\beta_{i,1}) \Gamma(\beta_{i,2})}{\Gamma(\rho_i^2 + 1)} = 1 \quad (17)$$

**Corollary 2.** *The PDF and CDF of Multi-hop RISE RF System which is the product of dGG are given as*

$$f_g(x) = \frac{1}{x} \psi_2 H_{0, 2K_2}^{2K_2, 0} \left[ U_2 x \mid \frac{-}{V_2} \right] \quad (18)$$

$$F_g(x) = \psi_2 H_{1, 2K_2+1}^{2K_2, 1} \left[ U_2 x \mid \frac{(1, 1)}{V_2, (0, 1)} \right] \quad (19)$$

where  $\psi_2 = \prod_{i=1}^{K_2} \frac{1}{\Gamma(\beta_{i,3})\Gamma(\beta_{i,4})}$ ,  $U_2 = \prod_{i=1}^{K_2} \left( \frac{\beta_{i,4}}{\alpha_{i,4}} \right)^{\frac{1}{\alpha_{i,4}}} \left( \frac{\beta_{i,3}}{\alpha_{i,3}} \right)^{\frac{1}{\alpha_{i,3}}}$  and  $V_2 = \{(\beta_{i,3}, \frac{1}{\alpha_{i,3}}), (\beta_{i,4}, \frac{1}{\alpha_{i,4}})\}_1^{K_2}$ .

*Proof:* A straight forward application of Theorem 1 completes the proof. ■

Using the IM/DD detector, we denote SNR of the cascaded FSO link as  $\gamma^{FSO} = \bar{\gamma}^{FSO}|h|^2$ , and the cascaded RF or R2V link as  $\gamma^{R2V} = \bar{\gamma}^{R2V}|g|^2$ , where  $\bar{\gamma}^{FSO} = \frac{P_1|h_l|^2}{\sigma_F^2}$  and  $\bar{\gamma}^{R2V} = \frac{P_2|g_l|^2}{\sigma_V^2}$  are the SNR terms without fading for the FSO and RF links, respectively. Here,  $h_l$  and  $g_l$  are the overall path gain of the cascaded FSO links and RF links.

In the following section, we analyze the system performance employing fixed-gain AF relaying to mix the FSO link with vehicular transmissions over RF.

#### IV. FIXED-GAIN AF RELAYING FOR HYBRID SYSTEM

We employ the fixed-gain AF relaying protocol with a gain  $G$  applied to the received FSO signal to forward the signal over RF for the desired vehicle. The gain selection can be entirely blind for a duration or using a semi-blind approach where it can be obtained using statistics of received signal power of the first hop (i.e., FSO link). The end-to-end SNR of the dual-hop system consisting of FSO and RF links is given by [46]:

$$\gamma^{AF} = \frac{\gamma^{FSO}\gamma^{R2V}}{\gamma^{R2V} + C} \quad (20)$$

where  $C = P_2/G^2\sigma_w^2$ . Using (20), the PDF of SNR for the fixed-gain AF relayed system is given by

$$f_{\gamma^{AF}}(\gamma) = \int_0^\infty f_{\gamma^{FSO}}\left(\frac{\gamma(x+C)}{x}\right) f_{\gamma^{R2V}}(x) \frac{x+C}{x} dx \quad (21)$$

where  $f_{\gamma^{FSO}}(\gamma)$  and  $f_{\gamma^{R2V}}(\gamma)$  are the PDF of SNR for FSO and RF links, respectively. We use (15) and (18) with a simple transformation of random variable to get the PDF of SNR for FSO  $f_{\gamma^{FSO}}(\gamma) = \frac{1}{2\sqrt{\gamma}\bar{\gamma}^{FSO}} f_h(\sqrt{\frac{\gamma}{\bar{\gamma}^{FSO}}})$  and RF link  $f_{\gamma^{R2V}}(\gamma) = \frac{1}{2\sqrt{\gamma}\bar{\gamma}^{R2V}} f_g(\sqrt{\frac{\gamma}{\bar{\gamma}^{R2V}}})$ .

To analyze performance of the fixed-gain AF relaying, analytical expressions of the PDF  $f_{\gamma}(\gamma)$  in (21) and the corresponding CDF  $F_{\gamma}(\gamma)$  is required.

**Lemma 1.** *The PDF and CDF of the fixed-gain AF relaying system in (21) is given as*

$$f_{\gamma^{AF}}(\gamma) = \frac{1}{4\gamma} \psi_1 \psi_2 H_{1,0:3K_1+1,K_1+1;0,2K_2+1}^{0,1;0,3K_1;2K_2+1,0} \left[ \begin{array}{c} U_1^{-1} \sqrt{\frac{\bar{\gamma}^{FSO}}{\gamma}} \\ U_2 \sqrt{\frac{C}{\bar{\gamma}^{R2V}}} \end{array} \middle| \begin{array}{c} (1 : \frac{1}{2}, \frac{1}{2}) : V_1; - \\ - : \{(-\rho_i^2, 1)\}_1^{K_2}, (1, \frac{1}{2}); V_2, (0, \frac{1}{2}) \end{array} \right] \quad (22)$$

$$F_{\gamma^{AF}}(\gamma) = \frac{1}{4} \psi_1 \psi_2 H_{1,0:3K_1+1,K_1+2;0,2K_2+1}^{0,1;1,3K_1;2K_2+1,0} \left[ \begin{array}{c} U_1^{-1} \sqrt{\frac{\bar{\gamma}^{FSO}}{\gamma}} \\ U_2 \sqrt{\frac{C}{\bar{\gamma}^{R2V}}} \end{array} \middle| \begin{array}{c} (1 : \frac{1}{2}, \frac{1}{2}) : V_1, (1, \frac{1}{2}); - \\ - : (0, \frac{1}{2}), \{(-\rho_i^2, 1)\}_1^{K_1}, (1, \frac{1}{2}); V_2, (0, \frac{1}{2}) \end{array} \right] \quad (23)$$

where  $V_1 = \{(1 - \beta_{i,1}, \frac{1}{\alpha_{i,1}}), (1 - \beta_{i,2}, \frac{1}{\alpha_{i,2}}), (1 - \rho_i^2, 1)\}_1^{K_1}$ ,  $V_2 = \{(\beta_{i,3}, \frac{1}{\alpha_{i,3}}), (\beta_{i,4}, \frac{1}{\alpha_{i,4}})\}_1^{K_2}$ .

*Proof:* We substitute PDF of FSO and RF links in (21), expand the definition of Fox-H function and interchange the order of integration to get

$$f_{\gamma^{AF}}(\gamma) = \frac{1}{4\gamma} \psi_1 \psi_2 \left( \frac{1}{2\pi j} \right)^2 \int_{\mathcal{L}_1} \int_{\mathcal{L}_2} \left( U_1 \sqrt{\frac{\gamma}{\bar{\gamma}^{FSO}}} \right)^{-n_1} \prod_{i=1}^{K_1} \Gamma(\beta_{i,2} + \frac{n_1}{\alpha_{i,2}}) \Gamma(\beta_{i,1} + \frac{n_1}{\alpha_{i,1}}) \frac{\Gamma(\rho_i^2 + n_1)}{\Gamma(\rho_i^2 + n_1 + 1)} \left( U_2 \sqrt{\frac{1}{\bar{\gamma}^{R2V}}} \right)^{-n_2} \prod_{i=1}^{K_2} \Gamma(\beta_{i,4} + \frac{n_2}{\alpha_{i,4}}) \Gamma(\beta_{i,3} + \frac{n_2}{\alpha_{i,3}}) \left( \int_0^\infty x^{-1-\frac{n_2}{2}} \left( \frac{x+C}{x} \right)^{-\frac{n_1}{2}} dx \right) dn_1 dn_2 \quad (24)$$

The inner integral can be solved using the identities [51, (3.194/3)] and [51, (8.384/1)] in terms of Gamma function:

$$\int_0^\infty x^{-1-\frac{n_2}{2}} \left( \frac{x+C}{x} \right)^{-\frac{n_1}{2}} dx = \frac{C^{-\frac{n_2}{2}} \Gamma(\frac{n_2}{2}) \Gamma(-\frac{n_2}{2} + \frac{n_1}{2})}{\Gamma(\frac{n_1}{2})} \quad (25)$$

We substitute (25) in (24) to get

$$f_{\gamma^{AF}}(\gamma) = \frac{1}{4\gamma} \psi_1 \psi_2 \left( \frac{1}{2\pi j} \right)^2 \int_{\mathcal{L}_1} \int_{\mathcal{L}_2} \left( U_1^{-1} \sqrt{\frac{\bar{\gamma}^{FSO}}{\gamma}} \right)^{n_1} \prod_{i=1}^{K_1} \Gamma(\beta_{i,2} + \frac{n_1}{\alpha_{i,2}}) \Gamma(\beta_{i,1} + \frac{n_1}{\alpha_{i,1}}) \frac{\Gamma(\rho_i^2 + n_1)}{\Gamma(\rho_i^2 + n_1 + 1)} \frac{1}{\Gamma(\frac{n_1}{2})} \left( U_2 \sqrt{\frac{C}{\bar{\gamma}^{R2V}}} \right)^{n_2} \prod_{i=1}^{K_2} \Gamma(\beta_{i,4} - \frac{n_2}{\alpha_{i,4}}) \Gamma(\beta_{i,3} - \frac{n_2}{\alpha_{i,3}}) \Gamma(-\frac{n_2}{2}) \Gamma(\frac{n_2}{2} + \frac{n_1}{2}) dn_1 dn_2 \quad (26)$$

and then apply the definition of bivariate Fox-H function to get (22).

To derived the CDF, we use (22) in  $F(\gamma) = \int_0^\gamma f(\gamma) d\gamma$ , apply the definition of Fox-H function to get

$$F_{\gamma^{AF}}(\gamma) = \frac{1}{4} \psi_1 \psi_2 \left( \frac{1}{2\pi j} \right)^2 \int_{\mathcal{L}_1} \int_{\mathcal{L}_2} \left( U_1^{-1} \sqrt{\frac{\bar{\gamma}^{FSO}}{\gamma}} \right)^{-n_1} \prod_{i=1}^{K_1} \Gamma(\beta_{i,2} - \frac{n_1}{\alpha_{i,2}}) \Gamma(\beta_{i,1} - \frac{n_1}{\alpha_{i,1}}) \frac{\Gamma(\rho_i^2 - n_1)}{\Gamma(\rho_i^2 - n_1 + 1)} \frac{1}{\Gamma(-\frac{n_1}{2})} \left( U_2 \sqrt{\frac{C}{\bar{\gamma}^{R2V}}} \right)^{n_2} \prod_{i=1}^{K_2} \Gamma(\beta_{i,4} - \frac{n_2}{\alpha_{i,4}}) \Gamma(\beta_{i,3} - \frac{n_2}{\alpha_{i,3}}) \Gamma(-\frac{n_2}{2}) \Gamma(\frac{n_2}{2} - \frac{n_1}{2}) \left( \int_0^\gamma t^{\frac{n_1}{2}-1} dt \right) dn_1 dn_2 \quad (27)$$

We solve the inner integral as  $\int_0^\gamma t^{\frac{n_1}{2}-1} dt = \gamma^{\frac{n_1}{2}} \frac{\gamma^{\frac{n_1}{2}}}{\gamma^{\frac{n_1}{2}}} = \gamma^{\frac{n_1}{2}} \frac{\gamma^{\frac{n_1}{2}}}{\gamma^{\frac{n_1}{2}}}$  and then use the definition of bivariate Fox-H function, to get (23), which completes the proof of Lemma. ■

Note that bivariate Fox's H-function has been extensively for the presentation of complicated fading distribution functions. Moreover, numerical computational codes are available in MATLAB for the computation of bivariate Fox's H-function.

$$\begin{aligned}
P_{\text{out}}^{AF,\infty} = & \frac{1}{4}\psi_1\psi_2 \left[ \sum_{i=1}^{K_1} \left( U_1^{-1} \sqrt{\frac{\gamma_{0,1}}{\gamma_{th}}} \right)^{-\alpha_{i,1}\beta_{i,1}} \prod_{i=1}^{K_1} \Gamma(\beta_{i,2} - \frac{\alpha_{i,1}\beta_{i,1}}{\alpha_{i,2}}) \frac{\Gamma(\rho_i^2 - \alpha_{i,1}\beta_{i,1})}{\Gamma(\rho_i^2 - \alpha_{i,1}\beta_{i,1} + 1)} \frac{\Gamma(\frac{\alpha_{i,1}\beta_{i,1}}{2})}{\Gamma(1 + \frac{\alpha_{i,1}\beta_{i,1}}{2})} \prod_{i=1}^{K_2} \Gamma(\beta_{i,4})\Gamma(\beta_{i,3}) \right. \\
& + \sum_{i=1}^{K_1} \left( U_1^{-1} \sqrt{\frac{\gamma_{0,1}}{\gamma_{th}}} \right)^{-\alpha_{i,2}\beta_{i,2}} \prod_{i=1}^{K_1} \Gamma(\beta_{i,1} - \frac{\alpha_{i,2}\beta_{i,2}}{\alpha_{i,1}}) \frac{\Gamma(\rho_i^2 - \alpha_{i,2}\beta_{i,2})}{\Gamma(\rho_i^2 - \alpha_{i,2}\beta_{i,2} + 1)} \frac{\Gamma(\frac{\alpha_{i,2}\beta_{i,2}}{2})}{\Gamma(1 + \frac{\alpha_{i,2}\beta_{i,2}}{2})} \prod_{i=1}^{K_2} \Gamma(\beta_{i,4})\Gamma(\beta_{i,3}) \\
& + \sum_{i=1}^{K_1} \left( U_1^{-1} \sqrt{\frac{\gamma_{0,1}}{\gamma_{th}}} \right)^{-\rho_i^2} \prod_{i=1}^{K_1} \Gamma(\beta_{i,2} - \frac{\rho_i^2}{\alpha_{i,2}}) \Gamma(\beta_{i,1} - \frac{\rho_i^2}{\alpha_{i,1}}) \frac{\Gamma(\frac{\rho_i^2}{2})}{\Gamma(1 + \frac{\rho_i^2}{2})} \prod_{i=1}^{K_2} \Gamma(\beta_{i,4})\Gamma(\beta_{i,3}) \\
& + \sum_{i=1}^{K_2} \left( U_2 \sqrt{\frac{C}{\gamma_{0,2}}} \right)^{\alpha_{i,3}\beta_{i,3}} \prod_{i=1}^{K_1} \Gamma(\beta_{i,2})\Gamma(\beta_{i,1}) \frac{\Gamma(\rho_i^2)}{\Gamma(\rho_i^2 + 1)} \prod_{i=1}^{K_2} \Gamma(\beta_{i,4} - \frac{\alpha_{i,3}\beta_{i,3}}{\alpha_{i,4}}) \Gamma(-\frac{\alpha_{i,3}\beta_{i,3}}{2}) \Gamma(\frac{\alpha_{i,3}\beta_{i,3}}{2}) \\
& + \sum_{i=1}^{K_2} \left( U_2 \sqrt{\frac{C}{\gamma_{0,2}}} \right)^{\alpha_{i,4}\beta_{i,4}} \prod_{i=1}^{K_1} \Gamma(\beta_{i,2})\Gamma(\beta_{i,1}) \frac{\Gamma(\rho_i^2)}{\Gamma(\rho_i^2 + 1)} \prod_{i=1}^{K_2} \Gamma(\beta_{i,3} - \frac{\alpha_{i,4}\beta_{i,4}}{\alpha_{i,3}}) \Gamma(-\frac{\alpha_{i,4}\beta_{i,4}}{2}) \Gamma(\frac{\alpha_{i,4}\beta_{i,4}}{2}) \left. \right] \quad (28)
\end{aligned}$$

In what follows, we use the results of Lemma 1 to present analytical expressions of outage probability, average BER, and ergodic capacity of the considered system.

#### A. Outage Probability

The outage probability of a system is a measure of SNR falling below certain threshold i.e.,  $P_{\text{out}} = Pr(\gamma \leq \gamma_{th}) = F_\gamma(\gamma_{th})$ . Thus, an exact outage probability for the mixed FSO-RF system can be obtained using  $\gamma = \gamma_{th}$  in the CDF formulation  $F_{\gamma^{AF}}(\gamma)$  of (23).

We use [52] to compute the residue of two Mellin-Barnes integrals of the corresponding bivariate Fox's H-function at the poles of (23) to develop the asymptotic expression in the high SNR regime, as given in (28). In order to get the diversity order  $G_{\text{out}}$  of the system, we express (28) as  $P_{\text{out}}^{AF,\infty} \propto \gamma_0^{-G_{\text{out}}}$ . Finally, selection of dominant terms in (28) provide the diversity order of the systems as  $G_{\text{out}} = \min \{ \{ \frac{\beta_{i,1}\alpha_{i,1}}{2}, \frac{\beta_{i,2}\alpha_{i,2}}{2}, \frac{\rho_i^2}{2} \}_{K_1}, \{ \frac{\beta_{i,3}\alpha_{i,3}}{2}, \frac{\beta_{i,4}\alpha_{i,4}}{2} \}_{K_2} \}$ . The diversity order depicts that the multi-hop performance depends on the link with the minimum of channel parameters. Thus, a performance degradation due to the channel fading and pointing errors can be compensated with an increase in the number of RISs for a given distance in both links.

#### B. Average BER

The average BER of a communication system with Gray coding using the CDF of the SNR is given as [53]:

$$\bar{P}_e = \frac{q^p}{2\Gamma(p)} \int_0^\infty \gamma^{p-1} e^{-q\gamma} F_\gamma(\gamma) d\gamma \quad (29)$$

where  $p$  and  $q$  are modulation specific parameters.

We substitute (23) in (29) and expand the definition of bivariate Fox-H function [50]:

$$\begin{aligned}
P_e^{AF} = & \frac{q^p}{8\Gamma(p)} \psi_1 \psi_2 \left( \frac{1}{2\pi j} \right)^2 \int_{\mathcal{L}_1} \int_{\mathcal{L}_2} (U_1^{-1} \sqrt{\gamma^{FSO}})^{n_1} \\
& (U_2 \sqrt{\frac{C}{\gamma^{RF}}})^{n_2} \prod_{i=1}^{K_1} \Gamma(\beta_{i,2} + \frac{n_1}{\alpha_{i,2}}) \Gamma(\beta_{i,1} + \frac{n_1}{\alpha_{i,1}}) \frac{\Gamma(\rho_i^2 + n_1)}{\Gamma(\rho_i^2 + n_1 + 1)} \\
& \frac{\Gamma(-\frac{n_1}{2})}{\Gamma(\frac{n_1}{2})\Gamma(1 - \frac{n_1}{2})} \prod_{i=1}^{K_2} \Gamma(\beta_{i,4} - \frac{n_2}{\alpha_{i,4}}) \Gamma(\beta_{i,3} - \frac{n_2}{\alpha_{i,3}}) \Gamma(-\frac{n_2}{2}) \\
& \Gamma(\frac{n_2}{2} + \frac{n_1}{2}) \left( \int_0^\infty \gamma^{p - \frac{n_1}{2} - 1} e^{-q\gamma} d\gamma \right) dn_1 dn_2 \quad (30)
\end{aligned}$$

We solve the inner integral in (30) as  $\int_0^\infty \gamma^{p - \frac{n_1}{2} - 1} e^{-q\gamma} d\gamma = \frac{\Gamma(p - \frac{n_1}{2})}{q^{p - \frac{n_1}{2}}}$  and apply the definition of bivariate Fox-H function to express BER of the AF system as

$$\begin{aligned}
P_e^{AF} = & \frac{1}{8\Gamma(p)} \psi_1 \psi_2 H_{1,0:3K_1+1,K_1+3;0,2K_2+1}^{0,1;2,3K_1;2K_2+1,0} \\
& \left[ \begin{array}{c} U_1^{-1} \sqrt{q\gamma^{FSO}} \\ U_2 \sqrt{\frac{C}{\gamma^{RF}}} \end{array} \middle| \begin{array}{c} (1 : \frac{1}{2}, \frac{1}{2}) : V_1, (1, \frac{1}{2}); - \\ - : (p, \frac{1}{2}), (0, \frac{1}{2}), \{(-\rho_i^2, 1)\}_1^{K_1}, (1, \frac{1}{2}); V_2, (0, \frac{1}{2}) \end{array} \right] \quad (31)
\end{aligned}$$

where  $V_1 = \{(1 - \beta_{i,1}, \frac{1}{\alpha_{i,1}}), (1 - \beta_{i,2}, \frac{1}{\alpha_{i,2}}), (1 - \rho_i^2, 1)\}_1^{K_1}$ ,  $V_2 = \{(\beta_{i,3}, \frac{1}{\alpha_{i,3}}), (\beta_{i,4}, \frac{1}{\alpha_{i,4}})\}_1^{K_2}$ .

Note that an asymptotic expression for the average BER can be derived using the similar procedure applied for the outage probability.

#### C. Ergodic Capacity

The ergodic capacity of a communication link over fading channels has the following representation:

$$\bar{\eta} = \int_0^\infty \log_2(1 + \gamma) f_\gamma(\gamma) d\gamma \quad (32)$$

$$\begin{aligned}
P_{\text{out}}^{\infty} = & \psi_1 \left[ \sum_{i=1}^{K_1} \alpha_{i,1} \frac{\prod_{j=1, j \neq i}^{K_1} \Gamma(\beta_{j,1} - \beta_{i,1} \frac{\alpha_{i,1}}{\alpha_{j,1}}) \prod_{j=1}^{K_1} \Gamma(\beta_{j,2} - \beta_{i,1} \frac{\alpha_{i,1}}{\alpha_{j,2}}) \prod_{j=1}^{K_1} \Gamma(\rho_j^2 - \beta_{i,1} \alpha_{i,1}) \Gamma(\beta_{i,1} \alpha_{i,1})}{\prod_{j=1}^{K_1} \Gamma(1 + \rho_j^2 - \beta_{i,1} \alpha_{i,1}) \Gamma(1 + \beta_{i,1} \alpha_{i,1})} \right. \\
& \left( \frac{U_1}{A_{0,i}} \sqrt{\frac{\gamma_{th}}{\bar{\gamma}^{FSO}}} \right)^{\beta_{i,1} \alpha_{i,1}} + \sum_{i=1}^{K_1} \alpha_{i,2} \frac{\prod_{j=1}^{K_1} \Gamma(\beta_{j,1} - \beta_{i,2} \frac{\alpha_{i,2}}{\alpha_{j,1}}) \prod_{j=1, j \neq i}^{K_1} \Gamma(\beta_{j,2} - \beta_{i,2} \frac{\alpha_{i,2}}{\alpha_{j,2}}) \prod_{j=1}^{K_1} \Gamma(\rho_j^2 - \beta_{i,2} \alpha_{i,2}) \Gamma(\beta_{i,2} \alpha_{i,2})}{\prod_{j=1}^{K_1} \Gamma(1 + \rho_j^2 - \beta_{i,2} \alpha_{i,2}) \Gamma(1 + \beta_{i,2} \alpha_{i,2})} \\
& \left( \frac{U_1}{A_{0,i}} \sqrt{\frac{\gamma_{th}}{\bar{\gamma}^{FSO}}} \right)^{\beta_{i,2} \alpha_{i,2}} + \sum_{i=1}^{K_1} \frac{\prod_{j=1}^{K_1} \Gamma(\beta_{j,1} - \frac{\rho_i^2}{\alpha_{j,1}}) \prod_{j=1}^{K_1} \Gamma(\beta_{j,2} - \frac{\rho_i^2}{\alpha_{j,2}}) \prod_{j=1, j \neq i}^{K_1} \Gamma(\rho_j^2 - \rho_i^2) \Gamma(\rho_i^2)}{\prod_{j=1}^{K_1} \Gamma(1 + \rho_j^2 - \rho_i^2) \Gamma(1 + \rho_i^2)} \left( \frac{U_1}{A_{0,i}} \sqrt{\frac{\gamma_{th}}{\bar{\gamma}^{FSO}}} \right)^{\rho_i^2} \Big] \\
& + \psi_2 \left[ \sum_{i=1}^{K_2} \alpha_{i,3} \frac{\prod_{j=1, j \neq i}^{K_2} \Gamma(\beta_{j,3} - \beta_{i,3} \frac{\alpha_{i,3}}{\alpha_{j,3}}) \prod_{j=1}^{K_2} \Gamma(\beta_{j,4} - \beta_{i,3} \frac{\alpha_{i,3}}{\alpha_{j,4}}) \Gamma(\beta_{i,3} \alpha_{i,3})}{\Gamma(1 + \beta_{i,3} \alpha_{i,3})} \left( U_2 \sqrt{\frac{\gamma_{th}}{\bar{\gamma}^{R2V}}} \right)^{\beta_{i,3} \alpha_{i,3}} \right. \\
& \left. + \sum_{i=1}^{K_2} \alpha_{i,4} \frac{\prod_{j=1}^{K_2} \Gamma(\beta_{j,3} - \beta_{i,4} \frac{\alpha_{i,4}}{\alpha_{j,3}}) \prod_{j=1, j \neq i}^{K_2} \Gamma(\beta_{j,4} - \beta_{i,4} \frac{\alpha_{i,4}}{\alpha_{j,4}}) \Gamma(\beta_{i,4} \alpha_{i,4})}{\Gamma(1 + \beta_{i,4} \alpha_{i,4})} \left( U_2 \sqrt{\frac{\gamma_{th}}{\bar{\gamma}^{R2V}}} \right)^{\beta_{i,4} \alpha_{i,4}} \right] \quad (36)
\end{aligned}$$

We substitute (22) in (32) and expand the definition of Fox-H function, to get

$$\eta^{\bar{A}F} = \frac{1}{4} \psi_1 \psi_2 \left( \frac{1}{2\pi j} \right)^2 \int_{\mathcal{L}_1} \int_{\mathcal{L}_2} (U_1^{-1} \sqrt{\bar{\gamma}^{FSO}})^{n_1} (U_2 \sqrt{\frac{C}{\bar{\gamma}^{R2V}}})^{n_2} F_{\gamma}^{DF}(\gamma) = F_{\gamma^{FSO}}(\gamma) + F_{\gamma^{R2V}}(\gamma) - F_{\gamma^{FSO}}(\gamma) F_{\gamma^{R2V}}(\gamma) \quad (37)$$

$$\begin{aligned}
& \prod_{i=1}^{K_1} \Gamma(\beta_{i,2} + \frac{n_1}{\alpha_{i,2}}) \Gamma(\beta_{i,1} + \frac{n_1}{\alpha_{i,1}}) \frac{\Gamma(\rho_i^2 + n_1)}{\Gamma(\rho_i^2 + n_1 + 1)} \frac{1}{\Gamma(\frac{n_1}{2})} \\
& \prod_{i=1}^{K_2} \Gamma(\beta_{i,4} - \frac{n_2}{\alpha_{i,4}}) \Gamma(\beta_{i,3} - \frac{n_2}{\alpha_{i,3}}) \Gamma(-\frac{n_2}{2}) \Gamma(\frac{n_2}{2} + \frac{n_1}{2}) \\
& \left( \int_0^{\infty} \gamma^{-1-\frac{n_1}{2}} \log_2(1+\gamma) d\gamma \right) dn_1 dn_2 \quad (33)
\end{aligned}$$

We solve the inner integral by expressing  $\ln(1+\gamma)$  in terms of Meijer-G function and use the identity [49, 07.34.21.0009.01],

$$\begin{aligned}
& \int_0^{\infty} \log_2(1+\gamma) \gamma^{(-\frac{n_1}{2}-1)} d\gamma = \\
& \log_2(e) \frac{\Gamma(-\frac{n_1}{2}) \Gamma(1 + \frac{n_1}{2}) \Gamma(-\frac{n_1}{2})}{\Gamma(1 - \frac{n_1}{2})} \quad (34)
\end{aligned}$$

We substitute (34) in (33) and apply the definition of bivariate Fox-H function, to get

$$\begin{aligned}
\eta^{\bar{A}F} = & \frac{\log_2(e)}{4} \psi_1 \psi_2 H_{1,0:3K_1+2,K_1+3;0,2K_2+1}^{0,1:2,3K_1+1;2K_2+1,0} \\
& \left[ \begin{array}{c} U_1^{-1} \sqrt{\bar{\gamma}^{FSO}} \\ U_2 \sqrt{\frac{C}{\bar{\gamma}^{R2V}}} \end{array} \middle| \begin{array}{c} (1 : \frac{1}{2}, \frac{1}{2}) : V_1, (0, \frac{1}{2}), (1, \frac{1}{2}); - \\ - : (0, \frac{1}{2}), (0, \frac{1}{2}), \{(-\rho_i^2, 1)\}_1^{K_1}, (1, \frac{1}{2}); V_2, (0, \frac{1}{2}) \end{array} \right] \quad (35)
\end{aligned}$$

where  $V_1 = \{(1 - \beta_{i,1}, \frac{1}{\alpha_{i,1}}), (1 - \beta_{i,2}, \frac{1}{\alpha_{i,2}}), (1 - \rho_i^2, 1)\}_1^{K_1}$ ,  $V_2 = \{(\beta_{i,3}, \frac{1}{\alpha_{i,3}}), (\beta_{i,4}, \frac{1}{\alpha_{i,4}})\}_1^{K_2}$ .

## V. DF RELAYING FOR HYBRID SYSTEM

Although the fixed-gain AF relaying is a simple technique to implement, it is desirable to analyze the performance of the near-optimal DF protocol as a benchmark.

Since  $\gamma^{FSO}$  and  $\gamma^{R2V}$  are independent, end-to-end SNR of DF relaying system is given as  $\gamma = \min\{\gamma^{FSO}, \gamma^{R2V}\}$ . Hence, the CDF of the SNR is

### A. Outage Probability

An exact outage probability for the mixed FSO-RF system can be obtained as  $P_{\text{out}}^{DF} = F_{\gamma}^{DF}(\gamma_{th})$ .

We use the asymptotic result of a single-variate Fox's H-function in [52, Th. 1.11] to express the outage probability in the high SNR regime, as given in (36). Using the dominant terms, the diversity order is  $G_{\text{out}}^{DF} = \min\{\{\frac{\beta_{i,1}\alpha_{i,1}}{2}, \frac{\beta_{i,2}\alpha_{i,2}}{2}, \frac{\rho_i^2}{2}\}_1^{K_1}, \{\frac{\beta_{i,3}\alpha_{i,3}}{2}, \frac{\beta_{i,4}\alpha_{i,4}}{2}\}_1^{K_2}\}$ . It can be seen that the diversity order using the average BER and outage probability has similar dependence on the channel and system parameters.

### B. Average BER

For the DF based dual-hop FSO-RF system, the average BER can be expressed using the average BER of individual links [54]:

$$\bar{P}_e = \bar{P}_e^{(FSO)} + \bar{P}_e^{(R2V)} - 2\bar{P}_e^{(FSO)} \bar{P}_e^{(R2V)} \quad (38)$$

where  $\bar{P}_e^{(FSO)}$  and  $\bar{P}_e^{(R2V)}$  are average BER of the cascaded FSO and cascaded RF links, respectively.

To derive  $\bar{P}_e^{(FSO)}$ , we substitute  $F_{\gamma^{FSO}}(\gamma)$  in (29), expand the definition of Fox-H function and then interchange the order of integration to get

$$\begin{aligned}
\bar{P}_e^{(FSO)} = & \frac{q^p}{2\Gamma(p)} \prod_{i=1}^{K_1} \frac{\rho_i^2}{\Gamma(\beta_{i,1}) \Gamma(\beta_{i,2})} \frac{1}{2\pi j} \int_{\mathcal{L}} \Gamma(\beta_{i,2} - \frac{n_1}{\alpha_{i,2}}) \\
& \Gamma(\beta_{i,1} - \frac{n_1}{\alpha_{i,1}}) \prod_{i=1}^{K_1} \left( \left( \frac{\beta_{i,2}}{\Omega_{i,2}} \right)^{\frac{1}{\alpha_{i,2}}} \left( \frac{\beta_{i,1}}{\Omega_{i,1}} \right)^{\frac{1}{\alpha_{i,1}}} \frac{1}{A_{0,i}} \sqrt{\frac{1}{\bar{\gamma}^{FSO}}} \right)^{n_1} \\
& \frac{\Gamma(\rho_i^2 - n_1)}{\Gamma(\rho_i^2 - n_1 + 1)} \frac{\Gamma(n_1)}{\Gamma(n_1 + 1)} \left( \int_0^{\infty} \gamma^{p+\frac{n_1}{2}-1} e^{-q\gamma} d\gamma \right) dn_1 \quad (39)
\end{aligned}$$

$$\bar{\eta}_1 = \frac{\log_2(e)}{2} \psi_1 H_{K_1+2,3K_1+2}^{3K_1+2,1} \left[ U_1 \sqrt{\frac{1}{\gamma^{FSO}}} \mid \left\{ (\beta_{i,1}, \frac{1}{\alpha_{i,1}}), (\beta_{i,2}, \frac{1}{\alpha_{i,2}}), (\rho_i^2, 1) \right\}_1^{K_1}, (0, \frac{1}{2}), (0, \frac{1}{2}) \right] \quad (42)$$

$$\bar{\eta}_2 = \frac{\log_2(e)}{2} \psi_2 H_{2,2K_2+2}^{2K_2+2,1} \left[ U_2 \sqrt{\frac{1}{\gamma^{R2V}}} \mid \left\{ (\beta_{i,3}, \frac{1}{\alpha_{i,3}}), (\beta_{i,4}, \frac{1}{\alpha_{i,4}}) \right\}_1^{K_2}, (0, \frac{1}{2}), (0, \frac{1}{2}) \right] \quad (43)$$

$$\bar{\eta}_{12} = \log_2(e) \psi_1 \psi_2 H_{3K_1, K_1+2, 2, 1, 2K_2+1}^{0, 3K_1+1, 2, 2K_2, 1} \left[ \begin{array}{c} U_1^{-2} \gamma^{FSO} \\ U_1^{-1} U_2 \sqrt{\frac{1}{\gamma^{R2V}}} \end{array} \mid \begin{array}{c} W_1 : (1, 1), (1, 1); (1, 1) \\ \{(-\rho_i^2 : 2, 1)\}_1^{K_1} : (1, 1), (0, 1); \{(\beta_{i,3}, \frac{1}{\alpha_{i,3}}), (\beta_{i,4}, \frac{1}{\alpha_{i,4}})\}_1^{K_2}, (0, 1) \end{array} \right] \quad (44)$$

$$\bar{\eta}_{21} = \log_2(e) \psi_1 \psi_2 H_{2K_2, 0, K_1+1, 3K_1+1, 2, 2}^{0, 2K_2, 3K_1, 1, 1, 2} \left[ \begin{array}{c} U_1 U_2^{-1} \sqrt{\frac{1}{\gamma^{R2V}}} \\ U_2^{-2} \gamma^{R2V} \end{array} \mid \begin{array}{c} W_2 : (1, 1), \{(1 + \rho_i^2, 1)\}_1^{K_1}; (1, 1), (1, 1) \\ - : \{(\beta_{i,1}, \frac{1}{\alpha_{i,1}}), (\beta_{i,2}, \frac{1}{\alpha_{i,2}}), (\rho_i^2, 1)\}_1^{K_1}, (0, 1); (1, 1), (0, 1) \end{array} \right] \quad (45)$$

where  $\psi_1 = \prod_{i=1}^{K_1} \frac{\rho_i^2}{\Gamma(\beta_{i,1})\Gamma(\beta_{i,2})}$ ,  $\psi_2 = \prod_{i=1}^{K_2} \frac{1}{\Gamma(\beta_{i,3})\Gamma(\beta_{i,4})}$ ,  $U_1 = \prod_{i=1}^{K_1} \frac{1}{A_{0,i}} \left( \frac{\beta_{i,2}}{\Omega_{i,2}} \right)^{\frac{1}{\alpha_{i,2}}} \left( \frac{\beta_{i,1}}{\Omega_{i,1}} \right)^{\frac{1}{\alpha_{i,1}}}$ ,  $U_2 = \prod_{i=1}^{K_2} \left( \frac{\beta_{i,4}}{\Omega_{i,4}} \right)^{\frac{1}{\alpha_{i,4}}} \left( \frac{\beta_{i,3}}{\Omega_{i,3}} \right)^{\frac{1}{\alpha_{i,3}}}$ ,  $W_1 = \{(1 - \beta_{i,1} : \frac{2}{\alpha_{i,1}}, \frac{1}{\alpha_{i,1}}), (1 - \beta_{i,2} : \frac{2}{\alpha_{i,2}}, \frac{1}{\alpha_{i,2}}), (1 - \rho_i^2 : 2, 1)\}_1^{K_1}$  and  $W_2 = \{(1 - \beta_{i,3} : \frac{1}{\alpha_{i,3}}, \frac{2}{\alpha_{i,3}}), (1 - \beta_{i,4} : \frac{1}{\alpha_{i,4}}, \frac{2}{\alpha_{i,4}})\}_1^{K_2}$ .

Using the inner integral  $\int_0^\infty \gamma^{p+\frac{n_1}{2}-1} e^{-q\gamma} d\gamma = \frac{\Gamma(p+\frac{n_1}{2})}{q^{p+\frac{n_1}{2}}}$  in (39), and applying the definition of Fox-H function to get

$$\bar{P}_e^{(FSO)} = \frac{\psi_1}{2\Gamma(p)} H_{K_1+2,3K_1+1}^{3K_1,2} \left[ \frac{U_1}{\sqrt{q\gamma^{FSO}}} \mid \begin{array}{c} (1, 1), V \\ V_1, (0, 1) \end{array} \right] \quad (40)$$

where  $\psi_1 = \prod_{i=1}^{K_1} \frac{\rho_i^2}{\Gamma(\beta_{i,1})\Gamma(\beta_{i,2})}$ ,  $U_1 = \prod_{i=1}^{K_1} \frac{1}{A_{0,i}} \left( \frac{\beta_{i,2}}{\Omega_{i,2}} \right)^{\frac{1}{\alpha_{i,2}}} \left( \frac{\beta_{i,1}}{\Omega_{i,1}} \right)^{\frac{1}{\alpha_{i,1}}}$ ,  $V = (1 - p, \frac{1}{2}), \{(\rho_i^2 + 1, 1)\}_1^{K_1}$  and  $V_1 = \{(\beta_{i,1}, \frac{1}{\alpha_{i,1}}), (\beta_{i,2}, \frac{1}{\alpha_{i,2}}), (\rho_i^2, 1)\}_1^{K_1}$ .

Similarly, the average BER of the RF link is:

$$\bar{P}_e^{(R2V)} = \frac{\psi_2}{2\Gamma(p)} H_{2,2K_2+1}^{2K_2,2} \left[ \frac{U_2}{\sqrt{q\gamma^{R2V}}} \mid \begin{array}{c} (1, 1), (1 - p, \frac{1}{2}) \\ V_2, (0, 1) \end{array} \right] \quad (41)$$

where  $\psi_2 = \prod_{i=1}^{K_2} \frac{1}{\Gamma(\beta_{i,3})\Gamma(\beta_{i,4})}$ ,  $U_2 = \prod_{i=1}^{K_2} \left( \frac{\beta_{i,4}}{\Omega_{i,4}} \right)^{\frac{1}{\alpha_{i,4}}} \left( \frac{\beta_{i,3}}{\Omega_{i,3}} \right)^{\frac{1}{\alpha_{i,3}}}$  and  $V_2 = \{(\beta_{i,3}, \frac{1}{\alpha_{i,3}}), (\beta_{i,4}, \frac{1}{\alpha_{i,4}})\}_1^{K_2}$ .

Since the average BER has a similar mathematical functional representation to the outage probability, we can use [52, Th. 1.11] to express average BER in the high SNR to get the diversity order  $G_{BER} = \min \{ \{ \frac{\beta_{i,1}\alpha_{i,1}}{2}, \frac{\beta_{i,2}\alpha_{i,2}}{2}, \frac{\rho_i^2}{2} \}_1^{K_1}, \{ \frac{\beta_{i,3}\alpha_{i,3}}{2}, \frac{\beta_{i,4}\alpha_{i,4}}{2} \}_1^{K_2} \}$ .

### C. Ergodic Capacity

We analyze the ergodic capacity of the dual-hop FSO-RF system by substituting the PDF of SNR  $f_{\gamma^{FSO}}^D(\gamma)$  (obtained by differentiating (37)) in (32). We denote  $\bar{\eta}_1 = \int_0^\infty \log_2(1+\gamma) f_{\gamma^{FSO}}(\gamma) d\gamma$ ,  $\bar{\eta}_2 = \int_0^\infty \log_2(1+\gamma) f_{\gamma^{R2V}}(\gamma) d\gamma$ ,  $\bar{\eta}_{12} = \int_0^\infty \log_2(1+\gamma) f_{\gamma^{FSO}}(\gamma) F_{\gamma^{R2V}}(\gamma) d\gamma$  and  $\bar{\eta}_{21} = \int_0^\infty \log_2(1+\gamma) f_{\gamma^{R2V}}(\gamma) F_{\gamma^{FSO}}(\gamma) d\gamma$ .

**Lemma 2.** An exact expression for the ergodic capacity of the considered system is given by

$$\bar{\eta} = \bar{\eta}_1 + \bar{\eta}_2 - \bar{\eta}_{12} - \bar{\eta}_{21} \quad (46)$$

where  $\bar{\eta}_1$ ,  $\bar{\eta}_2$ ,  $\bar{\eta}_{12}$ , and  $\bar{\eta}_{21}$  are given in (42), (43), (44) and (45) respectively.

*Proof:* Refer to Appendix B. ■

## VI. SIMULATION AND NUMERICAL RESULTS

In this section, we demonstrate the performance of multiple RIS empowered vehicular communications and validate the derived analytical expressions through numerical and Monte-Carlo simulations. We consider varying fading parameters to demonstrate the effect of the diversity order on the system performance. We assume that the backhaul FSO link length is 300 m and  $K_1 - 1$  optical RIS are deployed at equal distances. We model the FSO atmospheric turbulence using dGG parameters corresponding to strong turbulence (ST) ( $\alpha_1 = 1.8621, \alpha_2 = 1, \beta_1 = 0.5, \beta_2 = 1.8, \Omega_1 = 1.5074, \Omega_2 = 0.928$ ) and moderate turbulence (MT) ( $\alpha_1 = 2.169, \alpha_2 = 1, \beta_1 = 0.55, \beta_2 = 2.35, \Omega_1 = 1.5793, \Omega_2 = 0.9671$ ) [39]. We compute the effective path loss for FSO links for a visibility range of 3 Km [55] at a wavelength 1550 nm. The detector responsivity is 0.41 A/W and AWGN noise variance is taken as  $10^{-14}$  A<sup>2</sup>/GHz. We consider three pointing error (PE) scenarios: PE1, PE2, and PE3. In PE1, we assume that all the FSO links undergo the same pointing errors  $\rho = 2.5$ . In PE2, we use higher pointing error parameters ( $\rho = 1$  or  $\rho = 2.5$ ) from source to first optical RIS and last optical RIS to the relay and negligible pointing errors involving RIS to RIS due to a perfect beam alignment. In PE3, we use higher pointing error parameters ( $\rho = 1$  or  $\rho = 2.5$ ) from source to first optical RIS and last optical RIS to the relay and a lower pointing errors ( $\rho = 5$ ) involving RIS to RIS.

To illustrate the vehicular communications, we deploy  $K_2 - 1$  RIS at an equal distance placed perpendicular to the road. The distance between the relay and the last RF RIS is fixed at 100 m. To accommodate the mobility of vehicle in the performance analysis, we consider distance between the desired vehicle and the last RIS uniformly distributed between 1 m and 20 m. We use RF dGG parameters  $\alpha_3 = 1.5, \alpha_4 = 1, \beta_3 = 1.5, \beta_4 = 1.5, \Omega_3 = 1.5793, \Omega_4 = 0.9671$  to model the R2V link for vehicular transmissions [38]. We consider transmit and receive antenna gains as  $G_t = G_r = 35$  dB and a carrier frequency of 800 MHz for R2V transmissions. A noise floor of  $-104.4$  dBm is considered at the receiver of the



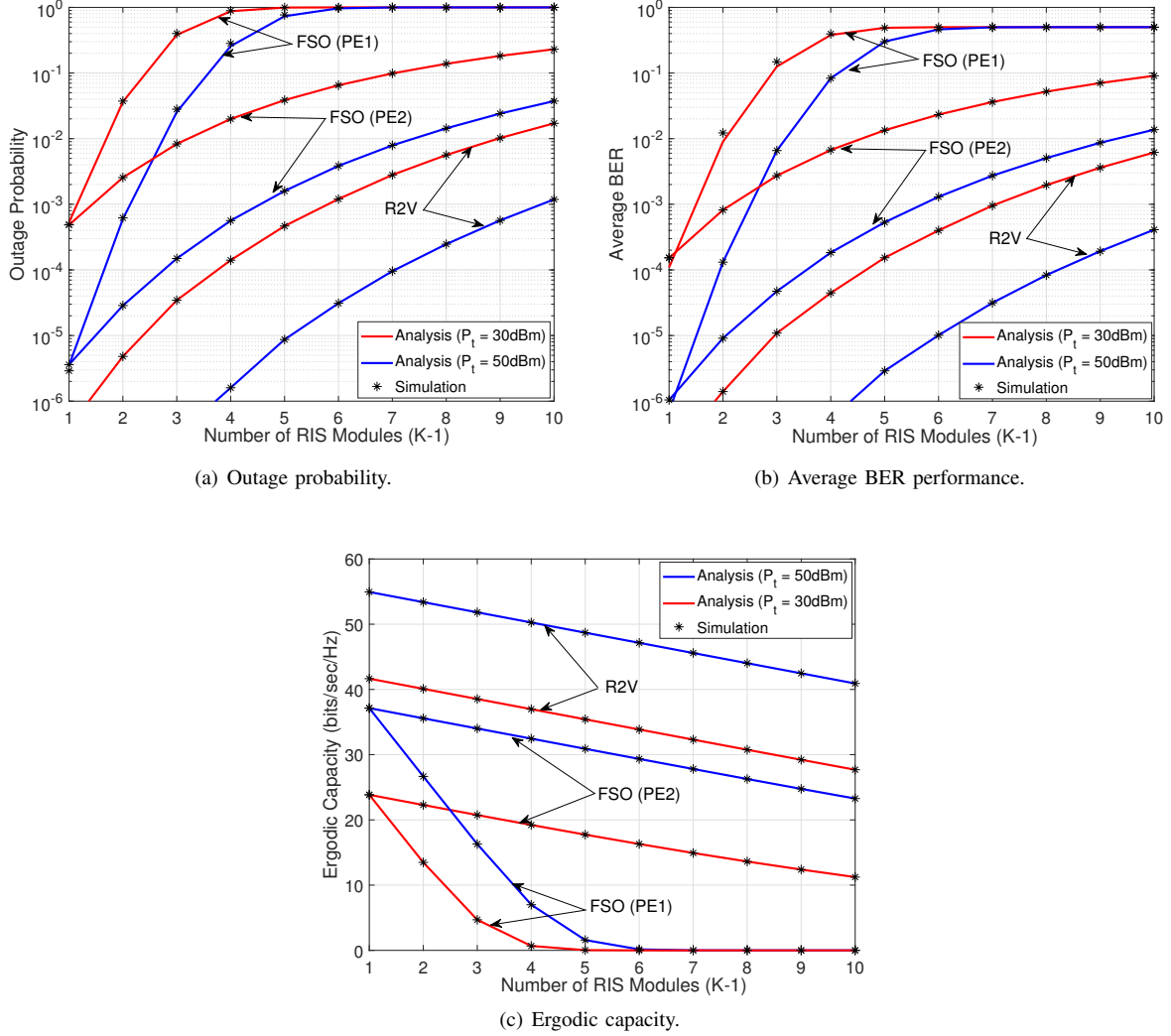


Fig. 2: Performance of multi-RIS transmissions for FSO and R2V links.

vehicle. A channel bandwidth of 20 MHz is used.

We demonstrate the effectiveness of multiple RISs for FSO (with moderate turbulence) and vehicular transmissions by plotting outage probability (in Fig. 2(a)), average BER (in Fig. 2(b)), and ergodic capacity (in Fig. 2(c)). Figures show the performance of multi-RIS system vs number of RISs ( $K - 1$  RISs constituting  $K$  hops) for FSO and R2V transmissions at a transmit power of  $P_t = 30$  dBm and  $P_t = 50$  dBm. It can be seen that an increase in the number of RIS modules between a source and destination decreases the performance, which can be regarded as a counter productive. However, without the use of multiple RIS, there exists no direct link which precludes any FSO transmissions and highly degraded R2V links. Thus, the use of multi-RIS should be limited enabling line-of-sight transmissions. Note that the reason for degradation in the performance with an increase in the number of RIS modules is the manifestation of cascading of channel coefficients comprising deterministic path gain ( $h_l < 1$ ).

First, Fig. 2a shows that an acceptable outage performance of  $10^{-3}$  can be obtained by deploying one and two RIS

modules in the PE1 scenario at the transmit power  $P_t = 30$  dBm and  $P_t = 50$  dBm, respectively. However, for the PE2 scenario, we can deploy upto 5 RIS modules at  $P_t = 50$  dBm to achieve an outage performance of  $10^{-3}$ . Thus, multi-hop optical RIS modules can improve the FSO system performance through the proper placing of RISs by increasing the number of RIS modules to reduce pointing errors. The figure also depicts that we can deploy 6 RIS (for a transmit power 30 dBm) and 10 RIS (for a transmit power 50 dBm) modules to achieve the outage performance of  $10^{-3}$  for vehicular communications. Moreover, a desirable performance can be achieved even at low transmit powers with a proper selection of the number of RISs. For example, an outage probability of  $10^{-4}$  is achievable with 4-RIS modules at  $P_t = 30$  dBm for R2V compared to 3 RISs at  $P_t = 50$  dBm for FSO transmissions with PE2 scenarios. Next, in Fig. 2(b), we plot the average BER of the multi-hop RIS FSO and R2V systems. The figure shows that the average BER performance provides a similar trend as observed with the outage probability. Finally, we plot the ergodic capacity in Fig. 2(c) for multi-hop RIS systems for three different

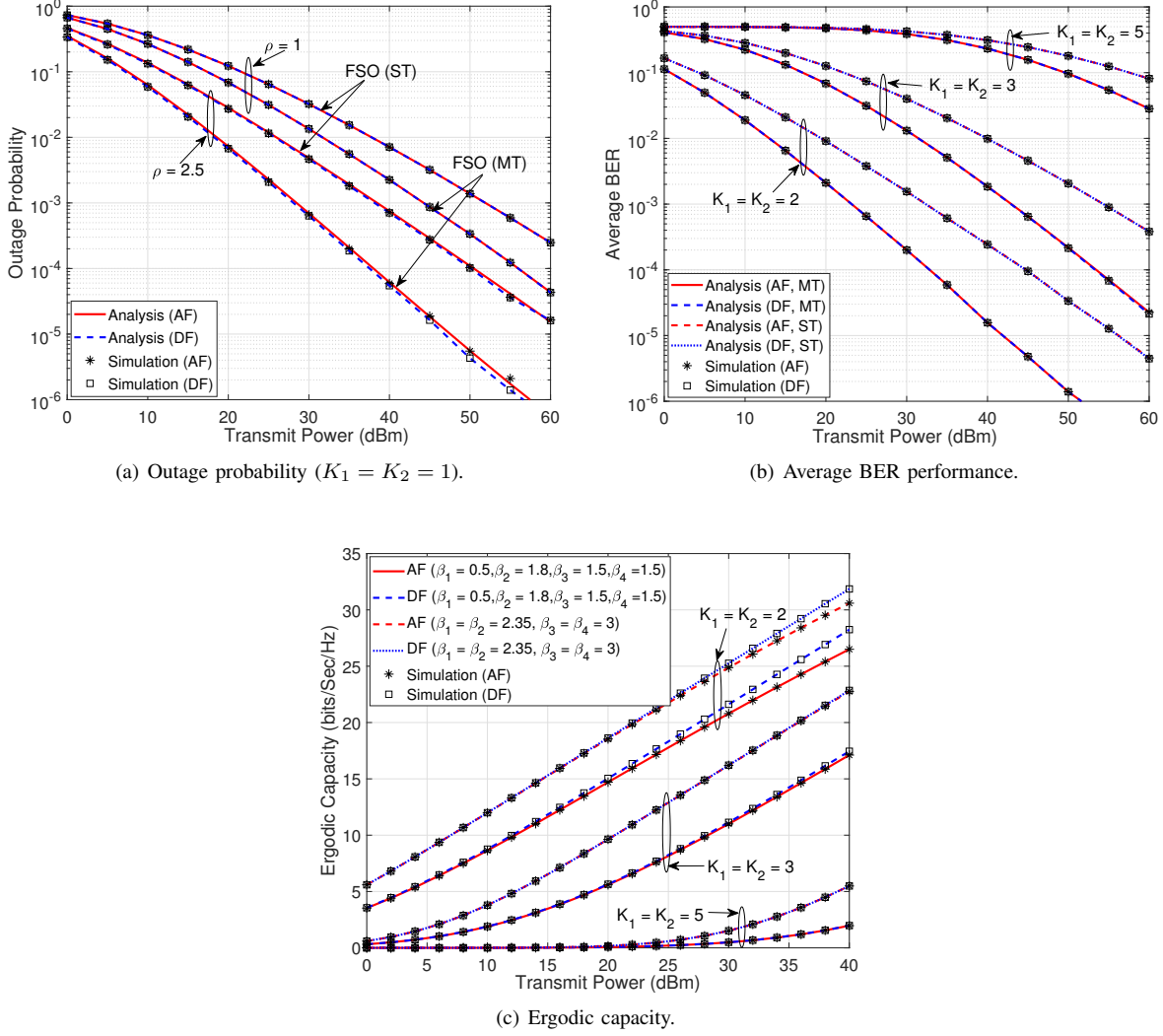


Fig. 3: Performance of RIS-assisted multi-hop FSO-R2V hybrid system.

scenarios. A higher channel capacity is possible with R2V since the link distance is short. Although cascading reduces the capacity, the effect of pointing errors and atmospheric turbulence can be mitigated by deploying multiple RIS to achieve LOS transmissions for FSO system. It can also be seen from Fig. 2(c) that a misalignment between RIS to RIS communication can be detrimental for the system performance and the channel capacity goes to zero with a few RIS modules. However, a single RIS module provides sufficient channel capacity (38 bps/Hz at 50 dBm) even when pointing errors are high in each hop of the FSO link.

In Fig. 3, we demonstrate the impact of multiple RIS modules on the performance of a hybrid FSO-RF system. First, we plot the outage probability as depicted in Fig. 3(a) for both DF and AF relay by considering a single RIS in both FSO and R2V links with different combinations of atmospheric turbulence (ST and MT) with PE3 pointing errors scenario for the FSO link and RF dGG parameters. It can be seen that strong turbulence requires an additional 10 dBm

of the transmit power compared with the moderate scenario to achieve an outage probability of  $10^{-3}$ . It can also be seen that the performance degrades with an increase in the pointing error requiring an additional 15 dBm of transmit power for the MT case when  $\rho$  is changed from 2.5 to 1. Moreover, the slope of the plots clearly demonstrates the diversity order of the system. For example, in the presence of ST turbulence,  $G_{\text{out}} = 0.46$  (obtained from the corresponding dGG parameter for the FSO link) is limited by the turbulence parameter irrespective of pointing errors  $\rho$  and R2V channel parameters. However, for the MT scenario, the diversity order is  $G_{\text{out}} = 0.5$  for  $\rho = 1$  (i.e., limited by pointing errors) and  $G_{\text{out}} = 0.59$  becomes independent of pointing errors when  $\rho = 2.5$ . Next, in Fig. 3(b), we demonstrate the average BER performance of the considered system for DBPSK modulation ( $p = 1, q = 1$ ). We consider both ST and MT turbulence for FSO links and the average BER is plotted for different number of hops considering an equal number of RIS modules in both FSO and R2V links. It can be seen that the performance

degrades with an increase in number of RIS modules due to the pointing errors in all the FSO links. The diversity order using the average BER of the system can be similarly inferred from the plots similar to the outage probability. Finally, we demonstrate the ergodic capacity in Fig. 3(c) for different fading parameters. It can be seen that there is a loss of about 10 bits/sec/Hz with an increase of  $K = 2$  to  $K = 3$  for the ST scenario. It can be seen from the figure that an increase in the parameter  $\beta$  improves the performance due to the decrease in the fading severity.

In all the plots, we validate our derived analytical results by numerically evaluating the Fox-H function with Monte-Carlo simulations. Further, the performance of the simpler AF relaying is equivalent to the near-optimal DF protocol for the hybrid FSO-RF system.

## VII. CONCLUSIONS

In this paper, we investigated the performance of a multiple RIS empowered mixed FSO-RF system for vehicular communications. We developed a framework to derive PDF and CDF of cascaded channels for generalized fading models. We employed AF and DF relaying protocols to mix two different technologies and analyzed the system performance by deriving analytical expressions for the outage probability, average BER, and ergodic capacity. To provide insights on the system performance, we also presented asymptotic analysis in the high SNR regime for the outage probability and demonstrated the impact of channel parameters on the diversity order of the system. We presented simulation results to show that the performance of the multiple RISs modules can provide line-of-sight propagation for FSO transmissions and reliable connection for vehicular communication. However, an excessive use of multiple RIS should be avoided since an increase in the number of RIS modules between a source and destination decreases the performance caused by the cascading of channel coefficients. We envision that the proposed work can be suitable for seamless connectivity in autonomous vehicular systems.

The proposed performance analysis can be extended with a statistical model for the mobility of vehicles and thereby joint optimization of placement for multiple RIS and throughput of the system to achieve a higher quality of service.

## APPENDIX A

We use Mellin transform to find the PDF of the product of  $K$  random variables as

$$f_X(x) = \frac{1}{x} \frac{1}{2\pi j} \int_{\mathcal{L}} \prod_{i=1}^K \mathbb{E}[X_i^r] x^{-r} dr \quad (47)$$

Substituting (12) in  $\mathbb{E}[X_i^n] = \int_0^\infty x^n f_{X_i}(x) dx$  and using the identity [50, 2.8], the  $r$ -th moment can be computed as

$$\begin{aligned} \mathbb{E}[X_i^r] &= \psi_i \int_0^\infty x^{r+\phi_i-1} H_{p,q}^{m,n} \left[ \zeta_i x \mid \begin{matrix} \{(a_{i,j}, A_{i,j})\}_{j=1}^p \\ \{(b_{i,j}, B_{i,j})\}_{j=1}^q \end{matrix} \right] dx \\ &= \psi_i \zeta_i^{-r-\phi_i} \frac{\prod_{j=1}^m \Gamma(b_{i,j} + B_{i,j}(r + \phi_i))}{\prod_{j=n+1}^p \Gamma(a_{i,j} + A_{i,j}(r + \phi_i))} \\ &\quad \frac{\prod_{j=1}^n \Gamma(1 - a_{i,j} - A_{i,j}(r + \phi_i))}{\prod_{j=m+1}^q \Gamma(1 - b_{i,j} - B_{i,j}(r + \phi_i))} \end{aligned} \quad (48)$$

Using (48) in (47), we get

$$\begin{aligned} f_X(x) &= \frac{1}{x} \prod_{i=1}^K \psi_i \zeta_i^{-\phi_i} \frac{1}{2\pi j} \int_{\mathcal{L}} \prod_{i=1}^K \left( \prod_{j=1}^m \zeta_i x \right)^{-r} \\ &\quad \frac{\prod_{j=1}^m \Gamma(b_{i,j} + B_{i,j}(r + \phi_i))}{\prod_{j=n+1}^p \Gamma(a_{i,j} + A_{i,j}(r + \phi_i))} \\ &\quad \frac{\prod_{j=1}^n \Gamma(1 - a_{i,j} - A_{i,j}(r + \phi_i))}{\prod_{j=m+1}^q \Gamma(1 - b_{i,j} - B_{i,j}(r + \phi_i))} dr \end{aligned} \quad (49)$$

We apply the definition of Fox-H function, to get (13). Using the (13) in  $F_X(x) = \int_0^x f_X(t) dt$ , an expression for the CDF:

$$\begin{aligned} F_X(x) &= \prod_{i=1}^K \psi_i \zeta_i^{-\phi_i} \frac{1}{2\pi j} \int_{\mathcal{L}} \left( \prod_{i=1}^K \zeta_i \right)^r \\ &\quad \frac{\prod_{j=1}^m \Gamma(b_{i,j} + B_{i,j}(-r + \phi_i))}{\prod_{j=n+1}^p \Gamma(a_{i,j} + A_{i,j}(-r + \phi_i))} \\ &\quad \frac{\prod_{j=1}^n \Gamma(1 - a_{i,j} - A_{i,j}(-r + \phi_i))}{\prod_{j=m+1}^q \Gamma(1 - b_{i,j} - B_{i,j}(-r + \phi_i))} \left( \int_0^x t^{-1+r} dt \right) dr \end{aligned} \quad (50)$$

Using the inner integral  $\int_0^x t^{-1+r} dt = \frac{x^r}{r} = x^r \frac{\Gamma(r)}{\Gamma(1+r)}$  in (50), and applying the definition of Fox-H function, we get (14).

## APPENDIX B

To derive  $\bar{\eta}_1$ , we use (15) to express

$$\begin{aligned} \bar{\eta}_1 &= \frac{1}{2} \prod_{i=1}^{K_1} \frac{\rho_i^2}{\Gamma(\beta_{i,1})\Gamma(\beta_{i,2})} \frac{1}{2\pi j} \int_{\mathcal{L}} \Gamma(\beta_{i,2} + \frac{n_1}{\alpha_{i,2}}) \Gamma(\beta_{i,1} + \frac{n_1}{\alpha_{i,1}}) \\ &\quad \prod_{i=1}^{K_1} \left( \left( \frac{\beta_{i,2}}{\Omega_{i,2}} \right)^{\frac{1}{\alpha_{i,2}}} \left( \frac{\beta_{i,1}}{\Omega_{i,1}} \right)^{\frac{1}{\alpha_{i,1}}} \frac{1}{A_{0,i}} \sqrt{\frac{1}{\bar{\gamma}^{FSO}}} \right)^{-n_1} \\ &\quad \frac{\Gamma(\rho_i^2 + n_1)}{\Gamma(\rho_i^2 + n_1 + 1)} \left( \int_0^\infty \gamma^{-1-\frac{n_1}{2}} \log_2(1 + \gamma) \right) dn_1 \end{aligned} \quad (51)$$

To solve the inner integral, we express  $\ln(1 + \gamma)$  in terms of Meijer-G function and use the identity [49, 07.34.21.0009.01],  $I = \frac{\Gamma(\frac{n_1}{2})\Gamma(1-\frac{n_1}{2})\Gamma(\frac{n_1}{2})}{\Gamma(1+\frac{n_1}{2})}$ , with the definition of Fox-H function to get (42). We follow the similar approach to derive  $\bar{\eta}_2$  in (43).

To derive  $\bar{\eta}_{12}$ , we use (15), (19) and express  $\ln(1 + \gamma)$  in terms of Meijer-G function to get

$$\begin{aligned} \eta_{12} &= \frac{\log_2(e)}{2} \psi_1 \psi_2 \int_0^\infty \gamma^{-1} G_{2,2}^{1,2} \left[ \gamma \mid \begin{matrix} 1, 1 \\ 1, 0 \end{matrix} \right] \\ &H_{K_1, 3K_1}^{3K_1, 0} \left[ U_1 \sqrt{\frac{\gamma}{\bar{\gamma}^{FSO}}} \mid \begin{matrix} \{(\rho_i^2 + 1, 1)\}_1^{K_1} \\ V_1 \end{matrix} \right] \\ &H_{1, 2K_2+1}^{2K_2, 1} \left[ U_2 \sqrt{\frac{\gamma}{\bar{\gamma}^{R2V}}} \mid \begin{matrix} (1, 1) \\ V_2, (0, 1) \end{matrix} \right] \end{aligned} \quad (52)$$

We then expand the definition of Meijer-G and Fox's-H function to get

$$\begin{aligned} \eta_{12} &= \frac{\log_2(e)}{2} \psi_1 \psi_2 \left( \frac{1}{2\pi j} \right)^2 \int_{\mathcal{L}} \int_{\mathcal{L}} \frac{\Gamma(u+1)\Gamma(-u)^2}{\Gamma(1-u)} \\ &\left( U_2 \sqrt{\frac{1}{\bar{\gamma}^{R2V}}} \right)^{-n_2} \prod_{i=1}^{K_2} \Gamma(\beta_{i,4} + \frac{n_2}{\alpha_{i,4}}) \Gamma(\beta_{i,3} + \frac{n_2}{\alpha_{i,3}}) \\ &\frac{\Gamma(-n_2)}{\Gamma(-n_2+1)} \left( \int_0^\infty \gamma^{-1-u-\frac{n_2}{2}} \right. \\ &\left. H_{K_1, 3K_1}^{3K_1, 0} \left[ U_1 \sqrt{\frac{\gamma}{\bar{\gamma}^{FSO}}} \mid \begin{matrix} \{(\rho_i^2 + 1, 1)\}_1^{K_1} \\ V_1 \end{matrix} \right] d\gamma \right) du dn_2 \end{aligned} \quad (53)$$

The inner is solved using the identity [50, 2.8] as

$$\begin{aligned} I &= 2 \left( \frac{U_1^2}{\bar{\gamma}^{FSO}} \right)^{u+\frac{n_2}{2}} \prod_{i=1}^{K_1} \Gamma(\beta_{i,1} + \frac{2}{\alpha_{i,1}}(u + \frac{n_2}{2})) \\ &\frac{\Gamma(\beta_{i,2} + \frac{2}{\alpha_{i,2}}(u + \frac{n_2}{2})) \Gamma(\rho_i^2 + 2(u + \frac{n_2}{2}))}{\Gamma(\rho_i^2 + 1 + 2(u + \frac{n_2}{2}))} \end{aligned} \quad (54)$$

We substitute (54) in (53) and apply the definition of bivariate Fox-H function to get (44). We follow the similar approach to derive  $\bar{\eta}_{21}$  in (45).

## REFERENCES

- [1] M. D. Renzo *et al.*, "Smart radio environments empowered by reconfigurable AI meta-surfaces: An idea whose time has come," *EURASIP J. Wireless Commun. Netw.*, vol. 2019, no. 129, May 2019.
- [2] E. Basar *et al.*, "Wireless communications through reconfigurable intelligent surfaces," *IEEE Access*, vol. 7, pp. 116753–116773, Aug. 2019.
- [3] Q. Wu *et al.*, "Intelligent reflecting surface aided wireless communications: A tutorial," *IEEE Trans. Commun.*, vol. 69, no. 5, pp. 3313–3351, Jan. 2021.
- [4] Y. Zhu *et al.*, "Intelligent reflecting surface-aided vehicular networks toward 6G: Vision, proposal, and future directions," *IEEE Veh. Technol. Mag.*, vol. 16, no. 4, pp. 2–10, Dec. 2021.
- [5] A. Trichili *et al.*, "Roadmap to free space optics," *J. Opt. Soc. Am. B*, vol. 37, no. 11, pp. A184–A201, Nov 2020.
- [6] A. U. Makarfi *et al.*, "Physical layer security in vehicular networks with reconfigurable intelligent surfaces," in *2020 IEEE 91st Veh. Tech. Conf. (VTC2020-Spring)*, May 2020, pp. 1–6.
- [7] N. Mensi *et al.*, "Physical layer security for V2I communications: Reflecting surfaces vs. relaying," [Online], arXiv: 2010.07216, 2020.
- [8] A. U. Makarfi *et al.*, "Reconfigurable intelligent surfaces-enabled vehicular networks: A physical layer security perspective," [Online], arXiv: 2004.11288, 2020.
- [9] J. Wang *et al.*, "Outage analysis for intelligent reflecting surface assisted vehicular communication networks," [Online], arXiv: 2004.08063, 2020.
- [10] D. Dampahalage *et al.*, "Intelligent reflecting surface aided vehicular communications," [Online], arXiv: 2011.03071, 2020.
- [11] L. Kong *et al.*, "Channel modeling and analysis of reconfigurable intelligent surfaces assisted vehicular networks," in *2021 IEEE Int. Conf. Commun. Workshops (ICC Workshops)*, Montreal, QC, Canada, June 2021, pp. 1–6.
- [12] K. Odeyemi *et al.*, "Reconfigurable intelligent surface assisted mobile network with randomly moving user over Fisher-Snedecor fading channel," *Physical Communication*, vol. 43, p. 101186, Aug. 2020.
- [13] Y. Chen *et al.*, "Resource allocation for intelligent reflecting surface aided vehicular communications," *IEEE Trans. Vehi. Technol.*, vol. 69, no. 10, pp. 12 321–12 326, Oct. 2020.
- [14] S. Li *et al.*, "Reconfigurable intelligent surface assisted UAV communication: Joint trajectory design and passive beamforming," *IEEE Wireless Commun. Lett.*, vol. 9, no. 5, pp. 716–720, May 2020.
- [15] L. Yang *et al.*, "On the performance of RIS-assisted dual-hop UAV communication systems," *IEEE Trans. Veh. Tech.*, vol. 69, no. 9, pp. 10 385–10 390, Sept. 2020.
- [16] D. Kudathanthirige *et al.*, "Performance analysis of intelligent reflective surfaces for wireless communication," in *ICC 2020-2020 IEEE Int. Conf. Commun. (ICC)*, Dublin, Ireland, July 2020, pp. 1–6.
- [17] A.-A. A. Boulgeorgos and A. Alexiou, "Performance analysis of reconfigurable intelligent surface-assisted wireless systems and comparison with relaying," *IEEE Access*, vol. 8, pp. 94 463–94 483, May 2020.
- [18] L. Yang *et al.*, "Accurate closed-form approximations to channel distributions of RIS-aided wireless systems," *IEEE Wireless Commun. Lett.*, vol. 9, no. 11, pp. 1985–1989, July 2020.
- [19] Q. Tao *et al.*, "Performance analysis of intelligent reflecting surface aided communication systems," *IEEE Commun. Lett.*, vol. 24, no. 11, pp. 2464–2468, July 2020.
- [20] R. C. Ferreira *et al.*, "Bit error probability for large intelligent surfaces under double-Nakagami fading channels," *IEEE Open J. Commun. Society*, vol. 1, pp. 750–759, May 2020.
- [21] D. Selimis *et al.*, "On the performance analysis of RIS-empowered communications over Nakagami-m fading," *IEEE Commun. Lett.*, vol. 25, no. 7, pp. 2191–2195, April 2021.
- [22] H. Ibrahim *et al.*, "Exact coverage analysis of intelligent reflecting surfaces with Nakagami-m channels," *IEEE Trans. Veh. Technol.*, vol. 70, no. 1, pp. 1072–1076, Jan. 2021.
- [23] I. Trigui *et al.*, "A comprehensive study of reconfigurable intelligent surfaces in generalized fading," [Online], arXiv: 2004.02922, 2020.
- [24] H. Du *et al.*, "Millimeter wave communications with reconfigurable intelligent surfaces: Performance analysis and optimization," *IEEE Trans. Commun.*, vol. 69, no. 4, pp. 2752–2768, Jan. 2021.
- [25] V. Jamali *et al.*, "Intelligent reflecting surface assisted free-space optical communications," *IEEE Commun. Magazine*, vol. 59, no. 10, pp. 57–63, Nov. 2021.
- [26] M. Najafi and R. Schober, "Intelligent reflecting surfaces for free space optical communications," in *2019 IEEE Global Commun. Conference (GLOBECOM)*, Waikoloa, HI, USA, Dec. 2019, pp. 1–7.
- [27] H. Wang *et al.*, "Performance of wireless optical communication with reconfigurable intelligent surfaces and random obstacles," arXiv:2001.05715, 2020.
- [28] L. Yang *et al.*, "Free-space optical communication with reconfigurable intelligent surfaces," ArXiv: 2012.00547, 2020.
- [29] A. R. Ndjongue *et al.*, "Performance analysis of RIS-based nT-FSO link over G-G turbulence with pointing errors," arXiv: 2102.03654, 2021.
- [30] V. K. Chapala and S. M. Zafaruddin, "Unified performance analysis of reconfigurable intelligent surface empowered free space optical communications," Accepted for publication in *IEEE Trans. Commun.*, Dec. 2021, arXiv: 2106.02000, 2021.
- [31] H. Du *et al.*, "Reconfigurable intelligent surface aided TeraHertz communications under misalignment and hardware impairments," [Online] arXiv: 2012.00267, 2020.
- [32] K. Dovelos *et al.*, "Intelligent reflecting surfaces at terahertz bands: channel modeling and analysis," [Online], arXiv: 2103.15239, 2021.
- [33] V. K. Chapala and S. M. Zafaruddin, "Exact Analysis of RIS-Aided THz Wireless Systems Over  $\alpha$ - $\mu$  Fading with Pointing Errors," *IEEE Commun. Lett.*, vol. 25, no. 11, pp. 3508–3512, Nov. 2021.
- [34] Y. U. Ozcan *et al.*, "Reconfigurable intelligent surfaces for the connectivity of autonomous vehicles," *IEEE Trans. Vehi. Technol.*, vol. 70, no. 3, pp. 2508–2513, March 2021.
- [35] C. Huang *et al.*, "Multi-hop RIS-empowered terahertz communications: A DRL-based hybrid beamforming design," *IEEE J. Sel. Areas Commun.*, vol. 39, no. 6, pp. 1663–1677, June 2021.
- [36] A.-A. A. Boulgeorgos *et al.*, "Cascaded composite turbulence and misalignment: Statistical characterization and applications to reconfigurable intelligent surface-empowered wireless systems," [Online], arXiv: 2106.15082, 2021.
- [37] M. A. Kashani *et al.*, "A novel statistical channel model for turbulence-induced fading in free-space optical systems," *Journal of Lightwave Technology*, vol. 33, no. 11, pp. 2303–2312, June 2015.

- [38] P. S. Bithas *et al.*, "On the double-generalized gamma statistics and their application to the performance analysis of V2V communications," *IEEE Trans. Commun.*, vol. 66, no. 1, pp. 448–460, Jan. 2018.
- [39] H. AlQuwaiee *et al.*, "On the performance of free-space optical communication systems over double Generalized Gamma channel," *IEEE J. Sel. Areas Commun.*, vol. 33, no. 9, pp. 1829–1840, Sept. 2015.
- [40] B. Ashrafzadeh *et al.*, "Unified performance analysis of multi-hop FSO systems over double generalized gamma turbulence channels with pointing errors," *IEEE Trans. Wirel. Commun.*, vol. 19, no. 11, pp. 7732–7746, Nov. 2020.
- [41] Z. Rahman *et al.*, "Performance of dual-hop relaying for OWC system over foggy channel with pointing errors and atmospheric turbulence," *IEEE Trans. Vehi. Technol.*, pp. 1–1, Dec. 2021.
- [42] L. Yang *et al.*, "Mixed dual-hop FSO-RF communication systems through reconfigurable intelligent surface," *IEEE Commun. Lett.*, vol. 24, no. 7, pp. 1558–1562, April 2020.
- [43] A. Sikri *et al.*, "Reconfigurable intelligent surface for mixed FSO-RF systems with co-channel interference," *IEEE Commun. Lett.*, vol. 25, no. 5, pp. 1605–1609, Feb. 2021.
- [44] A. M. Salhab and L. Yang, "Mixed RF/FSO relay networks: Ris-equipped rf source vs ris-aided rf source," *IEEE Wireless Commun. Lett.*, vol. 10, no. 8, pp. 1712–1716, Aug. 2021.
- [45] L. Yang *et al.*, "Indoor mixed dual-hop VLC/RF systems through reconfigurable intelligent surfaces," *IEEE Wireless Commun. Lett.*, vol. 9, no. 11, pp. 1995–1999, July 2020.
- [46] M. Hasna and M.-S. Alouini, "A performance study of dual-hop transmissions with fixed gain relays," *IEEE Trans. Wireless Commun.*, vol. 3, no. 6, pp. 1963–1968, Hong Kong, China, April 2004.
- [47] T. N. Do *et al.*, "Multi-ris-aided wireless systems: Statistical characterization and performance analysis," [Online], arXiv:2104.01912, Sept. 2021.
- [48] A. A. Farid and S. Hranilovic, "Outage capacity optimization for free-space optical links with pointing errors," *J. Lightw. Technol.*, vol. 25, no. 7, pp. 1702–1710, July 2007.
- [49] *The Wolfram function Site*, Accessed May 2021: <https://functions.wolfram.com/>.
- [50] A. Mathai *et al.*, *The H-Function: Theory and Applications*. Springer New York, 2009.
- [51] I. Gradshteyn *et al.*, *Table of Integrals, Series, And Products*, Jan. 2007.
- [52] A. Kilbas *et al.*, *H-Transforms: Theory and Applications*. CRC Press., Mar. 2004.
- [53] I. S. Ansari *et al.*, "A new formula for the BER of binary modulations with dual-branch selection over generalized-K composite fading channels," *IEEE Trans. Commun.*, vol. 59, no. 10, pp. 2654–2658, Oct. 2011.
- [54] T. A. Tsiftsis *et al.*, "Multihop free-space optical communications over strong turbulence channels," in *2006 IEEE Int. Conf. on Commun.*, vol. 6, Istanbul, Turkey, June 2006, pp. 2755–2759.
- [55] I. I. Kim *et al.*, "Comparison of laser beam propagation at 785 nm and 1550 nm in fog and haze for optical wireless communications," *Proc. SPIE*, vol. 4214, pp. 26–37, Nov. 2001.